

On an implicit return-mapping operator in Mohr-Coulomb plasticity and its derivation via subdifferential theory

S. Sysala¹, M. Cermak²

¹Institute of Geonics, Czech Academy of Sciences, Ostrava, Czech Republic

²VŠB–Technical University of Ostrava, Ostrava, Czech Republic

November 22, 2021

Abstract

The paper is devoted to the numerical solution of an elastoplastic constitutive initial value problem containing the Mohr-Coulomb yield criterion, a nonassociative plastic flow rule, and a nonlinear isotropic hardening. The constitutive problem is discretized by the implicit Euler method. Instead of the conventional Koiter formulations, we define the plastic flow rule using the subdifferential of the plastic potential to keep just one plastic multiplier and derive some formulas regardless a type of the return to the yield surface. This idea simplifies the solution scheme so that one can a priori decide about the return type even if the nonlinear hardening is introduced. Moreover, one can easily analyze the mathematical properties of the stress-strain operator and consequently simplify construction of the consistent tangent operator. These operators are used for solving the corresponding incremental boundary-value problem by the semismooth Newton method. The remaining part of the paper is focused on incremental limit analysis. The direct and also indirect controls of the loading process are considered and used in 2D and 3D numerical experiments on slope stability. The related Matlab codes are available.

Keywords: elastoplasticity, small-strain, Mohr-Coulomb yield surface, implicit return-mapping scheme, consistent tangent operator, semismooth Newton method, incremental limit analysis, slope stability

1 Introduction

Although plastic potentials are not essential parts of elastoplastic models, they are often used to formulate plastic flow rules. The definition of the potential, g , is closely related to the prescribed yield function, f , to be the model well-defined. For example, in associative plasticity, $g = f$. Within our work, we assume that g is a *convex and nonsmooth* function with respect to the variable $\boldsymbol{\sigma}$ representing the Cauchy stress tensor. Then the plastic flow rule reads (e.g. [1, Section 6.3.9]):

$$\dot{\boldsymbol{\epsilon}}^p \in \dot{\lambda} \partial_{\boldsymbol{\sigma}} g(\boldsymbol{\sigma}, A) \quad (1.1)$$

where, $\partial_{\boldsymbol{\sigma}} g(\boldsymbol{\sigma}, A)$ denotes the subdifferential of g at $(\boldsymbol{\sigma}, A)$ with respect to the stress variable. Further, $\dot{\boldsymbol{\epsilon}}^p$, $\dot{\lambda}$, and A denotes the plastic strain rate, the plastic multiplier rate, and the hardening thermodynamical forces, respectively. On the first sight, it seems that (1.1) is cumbersome for numerical treatment due to the presence of the multivalued flow direction. The main goal of our study is to show that *closed form* of $\partial_{\boldsymbol{\sigma}} g(\boldsymbol{\sigma}, A)$ is very useful for numerical treatment at least when the implicit Euler method is used for discretization of constitutive initial-value elastoplastic problems.

In [2], the formula (1.1) has been successfully used to simplify constitutive solution schemes for potentials that are isotropic and independent of the Lode angle. In this paper, we demonstrate that this idea can be extended on isotropic models formulated by the principal stress coordinates. To this end, we choose the model containing *the Mohr-Coulomb yield criterion, a nonassociative plastic flow rule and a nonlinear isotropic hardening*. Such model was studied, e.g., in [1] where the implicit return-mapping scheme and the consistent tangent operator were derived in detail. In comparison to this well-known reference, we straightforwardly simplify the solution scheme and derive useful properties of the discretized stress-strain operator. Such analysis of the operator enables, for example, to investigate its semismoothness [3, 4, 5, 6] or to find the consistent tangent operator in an easier form than in [1].

There exist many plastic yield criteria that are usually written by the principal stresses. Beside the Mohr-Coulomb one, we mention, for example, the Tresca [1] and the Hoek-Brown [7] criteria or the unified strength criterion [8]. The typical feature for such criteria is their *multisurface* representation. The Mohr-Coulomb yield criterion was chosen for our study since it is broadly exploited in soil and rock mechanics and has a relatively complex structure of singular points including edges and an apex. The Mohr-Coulomb models usually contain the nonassociative flow rule to catch the dilatant behavior of a material. Further, due to the presence of the nonlinear hardening, one cannot find the implicit constitutive solution in closed form, and thus the constitutive problem remains still challenging. As in [1], we let a hardening function in an abstract form. For a particular example of the nonlinear hardening in soil mechanics, we refer, e.g., [9].

In literature, there are many various concepts of the constitutive solution schemes or constructions of the consistent tangent operators for models containing yield criteria written in terms of the principal stresses. For their detailed overview and historical development, we refer the recent papers [7], and [10], respectively. First, it is worth mentioning that the solution concept depends on the formulation of the constitutive problem. In engineering practice, most concepts are based on the so-called Koiter formulations of the plastic flow rule suggested in [11] for associative models with multisurface yield criteria. Consequently, these formulations were extended also for nonassociative models, see, e.g., [12]. Unlike (1.1), Koiter's formulations contain various numbers of plastic multipliers depending on the position of σ on the yield surface. For the Mohr-Coulomb yield surface, one plastic multiplier is used for smooth portions, two multipliers for points on edges, and six multipliers for the apex. For each Koiter's formulation, one can derive a corresponding solution scheme more simply than for (1.1). However, only one solution scheme usually gives a correct solution since the position of the stress on the yield surface is not a priori known. Moreover, the handling with different numbers of plastic multipliers is not suitable for analysing the stress-strain operator even if the solution can be found in closed form. From the mathematical point of view, it is more convenient to formulate the constitutive problems using the principle of maximum plastic dissipation in case of associative plasticity [1, 13] or more generally, using the theory of bipotentials [14] including also some nonassociative models. These approaches enable variational formulations of the initial-boundary value elastoplastic problems. However, such treatment is out of the scope of this paper since we focus only on numerical solution of the discretized boundary value elastoplastic problems. For this purpose, the formulation (1.1) is sufficient and even more universal than the bipotential theory. Moreover, the corresponding solution scheme enriches and simplifies the current engineering practice, as we will see.

Secondly, the solution concept is dependent on discretization of constitutive problems. As it was mentioned, we focus on the (fully) implicit Euler method, which is one of the most popular discretization schemes in elastoplasticity. Beside other Euler-type methods (see, e.g., [1, 15]), the cutting plane methods are also popular. We refer [16] for the literature survey and recent development of these methods. When the constitutive problems are discretized by the implicit Euler methods, the solution is searched by the elastic predictor – plastic correction method. Within the plastic correction, the so-called (implicit) return-mapping scheme is constructed. For the Mohr-Coulomb

model, four types of the return are distinguished: return to the smooth portion, return to the “right” and “left” edges, and return to the apex, see, e.g., [1]. Such a distinction is necessary for the Koiter formulations but also useful for (1.1). It is worth mentioning that plastic correction problems can be reduced to problems formulated only in terms of the principal stress coordinates [17, 7, 1].

Since the discretized boundary value elastoplastic problems are mostly solved by nonsmooth variants of the Newton method [18, 3, 4, 5, 6], it is useful to construct the so-called consistent tangent operators representing a generalized derivative of the discretized stress-strain operators. To this end, we use the eigenprojections of symmetric second order tensors as in [19, 1]. A similar approach is also used in the recent book [14] with slightly different terminology like the spectral directions or the spin of a tensor. Another approach is introduced, e.g., in [20, 17, 7] where the consistent tangent operator is determined by the tangent operator representing the relation between the stress and strain rates.

To simplify numerical handling with the criteria given by the principal stresses, various approximative techniques have been suggested. These techniques are based on local or global smoothing of yields surfaces or plastic potentials. For literature survey, we refer [7, Section 1.2] or [21, 14, 9]. However, such an approach is out of the scope of this paper.

The rest of the paper is organized as it follows. Section 2 contains an auxiliary framework related to the subdifferential of an eigenvalue function and derivatives of eigenprojections. In Section 3, the Mohr-Coulomb constitutive initial value problem is formulated using (1.1). Section 4 is devoted to derivation of the improved solution scheme when the problem is discretized by the implicit Euler method. In Section 5, a simplified construction of the consistent tangent operator is introduced based on the results from the previous section. The incremental boundary value elastoplastic problem is discussed in Section 6. For purposes of the incremental limit analysis, two problems are formulated: with known and unknown values of the load factor. The former problem is used for a direct control of the loading process through the load factor while the latter for an indirect control. For both problems, the semismooth Newton method is introduced. Section 7 is devoted to numerical experiments related to slope stability problems in 2D and 3D. The paper also contains Appendix with some useful auxiliary results. In Appendix A, we derive derivatives of eigenprojections under plane strain assumptions to simplify the construction of the consistent tangent operator in such a case. In Appendix B, we derive algebraic representation for second and fourth order tensors within the 3D and plane strain problems.

In this paper, second order tensors, matrices, and vectors are denoted by bold letters. Further, the fourth order tensors are denoted by capital blackboard letters, e.g., \mathbb{D}_e or \mathbb{I} . The symbol \otimes means the tensor product [1]. We also use the following notation: $\mathbb{R}_+ := \{z \in \mathbb{R}; z \geq 0\}$ and $\mathbb{R}_{sym}^{3 \times 3}$ for the space of symmetric, second order tensors. The standard scalar product in \mathbb{R}^3 and the biscalar product in $\mathbb{R}_{sym}^{3 \times 3}$ are denoted as \cdot and $;$, respectively.

2 Spectral decomposition of a second order tensor

This section contains mainly preliminaries related to the spectral decomposition and derivatives of eigenvalues and eigenprojections. We complete these known results with derivation of the subdifferential of an eigenvalue function. Its knowledge will be crucial to simplify the return-mapping scheme of the Mohr-Coulomb model.

Consider a tensor $\boldsymbol{\sigma} \in \mathbb{R}_{sym}^{3 \times 3}$ and its spectral decomposition:

$$\boldsymbol{\sigma} = \sum_{i=1}^3 \sigma_i \mathbf{e}_i \otimes \mathbf{e}_i, \quad \sigma_1 \geq \sigma_2 \geq \sigma_3, \quad (2.1)$$

where $\sigma_i \in \mathbb{R}$, $\mathbf{e}_i \in \mathbb{R}^3$, $i = 1, 2, 3$, denote the eigenvalues, and the eigenvectors of $\boldsymbol{\sigma}$, respectively. The eigenvalues $\sigma_1, \sigma_2, \sigma_3$ can be standardly computed using the Haigh-Westergaard coordinates,

see e.g. [1, Appendix A], and are uniquely determined with respect to the prescribed ordering. Let $\omega_1, \omega_2, \omega_3$ denote the corresponding eigenvalue functions, i.e. $\sigma_i := \omega_i(\boldsymbol{\sigma})$, $i = 1, 2, 3$. Further, we consider the following set of admissible eigenvectors of $\boldsymbol{\sigma}$:

$$V(\boldsymbol{\sigma}) := \{(\mathbf{e}_1, \mathbf{e}_2, \mathbf{e}_3) \in \mathbb{R}^3 \times \mathbb{R}^3 \times \mathbb{R}^3 \mid \mathbf{e}_i \cdot \mathbf{e}_j = \delta_{ij}; \boldsymbol{\sigma} \mathbf{e}_i = \sigma_i \mathbf{e}_i, i, j = 1, 2, 3; \sigma_1 \geq \sigma_2 \geq \sigma_3\}.$$

2.1 Subdifferential of an eigenvalue function

Recall another definition of the maximal and minimal eigenvalue functions:

$$\omega_1(\boldsymbol{\sigma}) = \max_{\substack{\mathbf{e} \in \mathbb{R}^3 \\ |\mathbf{e}|=1}} \boldsymbol{\sigma} : (\mathbf{e} \otimes \mathbf{e}) = \max_{\substack{\mathbf{e} \in \mathbb{R}^3 \\ |\mathbf{e}|=1}} (\boldsymbol{\sigma} \mathbf{e}) \cdot \mathbf{e}, \quad \omega_3(\boldsymbol{\sigma}) = \min_{\substack{\mathbf{e} \in \mathbb{R}^3 \\ |\mathbf{e}|=1}} \boldsymbol{\sigma} : (\mathbf{e} \otimes \mathbf{e}), \quad (2.2)$$

and define the function

$$g(\boldsymbol{\sigma}) := a\omega_1(\boldsymbol{\sigma}) - b\omega_3(\boldsymbol{\sigma}), \quad a, b \geq 0, \quad \boldsymbol{\sigma} \in \mathbb{R}_{sym}^{3 \times 3}. \quad (2.3)$$

Using (2.2), one can easily check that g is a convex function in $\mathbb{R}_{sym}^{3 \times 3}$. Therefore, one can introduce the subdifferential of g at any $\boldsymbol{\sigma} \in \mathbb{R}_{sym}^{3 \times 3}$:

$$\partial g(\boldsymbol{\sigma}) = \{\boldsymbol{\nu} \in \mathbb{R}_{sym}^{3 \times 3} \mid g(\boldsymbol{\tau}) \geq g(\boldsymbol{\sigma}) + \boldsymbol{\nu} : (\boldsymbol{\tau} - \boldsymbol{\sigma}) \quad \forall \boldsymbol{\tau} \in \mathbb{R}_{sym}^{3 \times 3}\}.$$

It holds the following result.

Lemma 2.1. *For any $\boldsymbol{\sigma} \in \mathbb{R}_{sym}^{3 \times 3}$,*

$$\partial g(\boldsymbol{\sigma}) = \left\{ \boldsymbol{\nu} = \sum_{i=1}^3 \nu_i \mathbf{e}_i \otimes \mathbf{e}_i \in \mathbb{R}_{sym}^{3 \times 3} \mid (\mathbf{e}_1, \mathbf{e}_2, \mathbf{e}_3) \in V(\boldsymbol{\sigma}); a \geq \nu_1 \geq \nu_2 \geq \nu_3 \geq -b; \sum_{i=1}^3 \nu_i = a - b; (\nu_1 - a)[\omega_1(\boldsymbol{\sigma}) - \omega_2(\boldsymbol{\sigma})] = 0; (\nu_3 + b)[\omega_2(\boldsymbol{\sigma}) - \omega_3(\boldsymbol{\sigma})] = 0 \right\}. \quad (2.4)$$

Proof. Since $g(\mathbf{0}) = 0$ and $g(2\boldsymbol{\sigma}) = 2g(\boldsymbol{\sigma})$ we obtain

$$\partial g(\boldsymbol{\sigma}) = \{\boldsymbol{\nu} \in \mathbb{R}_{sym}^{3 \times 3} \mid g(\boldsymbol{\sigma}) = \boldsymbol{\nu} : \boldsymbol{\sigma}; g(\boldsymbol{\tau}) \geq \boldsymbol{\nu} : \boldsymbol{\tau} \quad \forall \boldsymbol{\tau} \in \mathbb{R}_{sym}^{3 \times 3}\}. \quad (2.5)$$

First, we derive necessary and sufficient conditions ensuring

$$g(\boldsymbol{\tau}) \geq \boldsymbol{\nu} : \boldsymbol{\tau} \quad \forall \boldsymbol{\tau} \in \mathbb{R}_{sym}^{3 \times 3} \quad (2.6)$$

for some $\boldsymbol{\nu} \in \mathbb{R}_{sym}^{3 \times 3}$. Consider the following spectral decomposition of $\boldsymbol{\nu}$:

$$\boldsymbol{\nu} = \sum_{i=1}^3 \nu_i \mathbf{f}_i \otimes \mathbf{f}_i, \quad \nu_1 \geq \nu_2 \geq \nu_3, \quad (\mathbf{f}_1, \mathbf{f}_2, \mathbf{f}_3) \in V(\boldsymbol{\nu}). \quad (2.7)$$

Choose $\boldsymbol{\tau} = \pm \mathbf{I}$, where \mathbf{I} is the unit tensor in $\mathbb{R}_{sym}^{3 \times 3}$. Then from (2.6) we have

$$\nu_1 + \nu_2 + \nu_3 = a - b. \quad (2.8)$$

Choose $\boldsymbol{\tau} = \mathbf{f}_1 \otimes \mathbf{f}_1$ and $\boldsymbol{\tau} = -\mathbf{f}_3 \otimes \mathbf{f}_3$. Then from (2.6) we have, respectively,

$$\nu_1 \leq a, \quad \nu_3 \geq -b. \quad (2.9)$$

Let $\boldsymbol{\tau} \in \mathbb{R}_{sym}^{3 \times 3}$ be arbitrarily chosen, denote $\tau_i := \boldsymbol{\tau} : (\mathbf{f}_i \otimes \mathbf{f}_i)$, $i = 1, 2, 3$ and consider the following reordering of τ_i and ν_i , $i = 1, 2, 3$:

$$\tau_k \geq \tau_l \geq \tau_m, \quad k \neq l \neq m \neq k \quad \implies \quad \tilde{\tau}_1 = \tau_k, \quad \tilde{\tau}_2 = \tau_l, \quad \tilde{\tau}_3 = \tau_m, \quad \tilde{\nu}_1 = \nu_k, \quad \tilde{\nu}_2 = \nu_l, \quad \tilde{\nu}_3 = \nu_m.$$

Then $\tilde{\tau}_1 \geq \tilde{\tau}_2 \geq \tilde{\tau}_3$, $\tilde{\nu}_1 \leq \nu_1$, $\tilde{\nu}_3 \geq \nu_3$ and

$$\begin{aligned} \boldsymbol{\nu} : \boldsymbol{\tau} &= \sum_{i=1}^3 \nu_i \tau_i = \sum_{i=1}^3 \tilde{\nu}_i \tilde{\tau}_i = \tilde{\nu}_1(\tilde{\tau}_1 - \tilde{\tau}_2) + (\tilde{\nu}_1 + \tilde{\nu}_2)(\tilde{\tau}_2 - \tilde{\tau}_3) + (\tilde{\nu}_1 + \tilde{\nu}_2 + \tilde{\nu}_3)\tilde{\tau}_3 \\ &\stackrel{(2.8)}{=} \tilde{\nu}_1(\tilde{\tau}_1 - \tilde{\tau}_2) + (a - b - \tilde{\nu}_3)(\tilde{\tau}_2 - \tilde{\tau}_3) + (a - b)\tilde{\tau}_3 \\ &\leq \nu_1(\tilde{\tau}_1 - \tilde{\tau}_2) + (a - b - \nu_3)(\tilde{\tau}_2 - \tilde{\tau}_3) + (a - b)\tilde{\tau}_3 \\ &\stackrel{(2.9)}{\leq} a(\tilde{\tau}_1 - \tilde{\tau}_2) + a(\tilde{\tau}_2 - \tilde{\tau}_3) + (a - b)\tilde{\tau}_3 = a\tilde{\tau}_1 - b\tilde{\tau}_3 \\ &= a \max_i \boldsymbol{\tau} : (\mathbf{f}_i \otimes \mathbf{f}_i) - b \min_i \boldsymbol{\tau} : (\mathbf{f}_i \otimes \mathbf{f}_i) \leq a \max_{|\mathbf{e}|=1} \boldsymbol{\tau} : (\mathbf{e} \otimes \mathbf{e}) - b \min_{|\mathbf{e}|=1} \boldsymbol{\tau} : (\mathbf{e} \otimes \mathbf{e}) \\ &= a\omega_1(\boldsymbol{\tau}) - b\omega_3(\boldsymbol{\tau}) = g(\boldsymbol{\tau}) \quad \forall \boldsymbol{\tau} \in \mathbb{R}_{sym}^{3 \times 3}. \end{aligned} \quad (2.10)$$

Thus the conditions (2.7)-(2.9) are necessary and sufficient for (2.6).

Second, assume that $\boldsymbol{\nu}$ belongs to $\partial g(\boldsymbol{\sigma})$ and satisfies (2.7)-(2.9). Since $g(\boldsymbol{\sigma}) \stackrel{(2.5)}{=} \boldsymbol{\nu} : \boldsymbol{\sigma}$, the equalities must hold in (2.10) for $\boldsymbol{\tau} = \boldsymbol{\sigma}$, i.e., we have:

$$\tilde{\nu}_1(\tilde{\tau}_1 - \tilde{\tau}_2) = \nu_1(\tilde{\tau}_1 - \tilde{\tau}_2) = a(\tilde{\tau}_1 - \tilde{\tau}_2), \quad (a - b - \tilde{\nu}_3)(\tilde{\tau}_2 - \tilde{\tau}_3) = (a - b - \nu_3)(\tilde{\tau}_2 - \tilde{\tau}_3) = a(\tilde{\tau}_2 - \tilde{\tau}_3), \quad (2.11)$$

$$a[\tilde{\tau}_1 - \omega_1(\boldsymbol{\sigma})] = 0, \quad b[\tilde{\tau}_3 - \omega_3(\boldsymbol{\sigma})] = 0. \quad (2.12)$$

From (2.7), (2.8) and (2.11), we have $\tilde{\nu}_i = \nu_i$, $\tilde{\tau}_i = \tau_i$, $i = 1, 2, 3$. Therefore, (2.11) and (2.12) reduce into

$$(\nu_1 - a)(\tau_1 - \tau_2) = 0, \quad (\nu_3 + b)(\tau_2 - \tau_3) = 0, \quad (2.13)$$

$$a[\tau_1 - \omega_1(\boldsymbol{\sigma})] = 0, \quad b[\tau_3 - \omega_3(\boldsymbol{\sigma})] = 0, \quad (2.14)$$

If $a, b > 0$ then from (2.14) we have $\tau_1 = \max_i \boldsymbol{\sigma} : (\mathbf{f}_i \otimes \mathbf{f}_i) = \omega_1(\boldsymbol{\sigma})$ and $\tau_3 = \min_i \boldsymbol{\sigma} : (\mathbf{f}_i \otimes \mathbf{f}_i) = \omega_3(\boldsymbol{\sigma})$. Hence, $\boldsymbol{\sigma} \mathbf{f}_1 = \omega_1(\boldsymbol{\sigma}) \mathbf{f}_1$, $\boldsymbol{\sigma} \mathbf{f}_3 = \omega_3(\boldsymbol{\sigma}) \mathbf{f}_3$ and, consequently, one can easily derive $\boldsymbol{\sigma} \mathbf{f}_2 = \omega_2(\boldsymbol{\sigma}) \mathbf{f}_2$. This implies $(\mathbf{f}_1, \mathbf{f}_2, \mathbf{f}_3) \in V(\boldsymbol{\sigma})$ and thus

$$V(\boldsymbol{\nu}) \cap V(\boldsymbol{\sigma}) \neq \emptyset. \quad (2.15)$$

Further, (2.15) holds even if $a = 0$ or $b = 0$. For the sake of brevity, we prove it only for the case $a = 0$ and $b > 0$. For the remaining cases, the proof of (2.15) is similar. From $b > 0$, we have again $\tau_3 = \omega_3(\boldsymbol{\sigma})$ and $\boldsymbol{\sigma} \mathbf{f}_3 = \omega_3(\boldsymbol{\sigma}) \mathbf{f}_3$. The assumption $a = 0$ implies that $\nu_1 = 0$ and $\nu_2 + \nu_3 = -b$ making use (2.8)-(2.9). If $\nu_3 = -b$ then $\nu_2 = 0$ and thus $\boldsymbol{\nu} = -b \mathbf{f}_3 \otimes \mathbf{f}_3$. Therefore, one can choose $\mathbf{f}_1, \mathbf{f}_2$ such that (2.15) holds. Conversely, if $\nu_3 > -b$ then $\tau_2 \stackrel{(2.13)}{=} \tau_3 = \omega_3(\boldsymbol{\sigma})$. Hence, $\boldsymbol{\sigma} \mathbf{f}_2 = \omega_3(\boldsymbol{\sigma}) \mathbf{f}_2$ and consequently $\boldsymbol{\sigma} \mathbf{f}_1 = \omega_1(\boldsymbol{\sigma}) \mathbf{f}_1$ proving (2.15).

Thus, one can write any element $\boldsymbol{\nu}$ from $\partial g(\boldsymbol{\sigma})$ in the form $\boldsymbol{\nu} = \sum_{i=1}^3 \nu_i \mathbf{f}_i \otimes \mathbf{f}_i$, where $(\mathbf{f}_1, \mathbf{f}_2, \mathbf{f}_3) \in V(\boldsymbol{\nu}) \cap V(\boldsymbol{\sigma})$. For such a choice of \mathbf{f}_i , we receive $\tau_i = \omega_i(\boldsymbol{\sigma})$, $i = 1, 2, 3$, and from (2.13) we have

$$(\nu_1 - a)[\omega_1(\boldsymbol{\sigma}) - \omega_2(\boldsymbol{\sigma})] = 0, \quad (\nu_3 + b)[\omega_2(\boldsymbol{\sigma}) - \omega_3(\boldsymbol{\sigma})] = 0. \quad (2.16)$$

We have proven that for any element $\boldsymbol{\nu} \in \partial g(\boldsymbol{\sigma})$ the conditions (2.7)-(2.9), (2.15) and (2.16) hold. Since $V(\boldsymbol{\nu}) \cap V(\boldsymbol{\sigma}) \subset V(\boldsymbol{\sigma})$,

$$\partial g(\boldsymbol{\sigma}) \subset \left\{ \boldsymbol{\nu} = \sum_{i=1}^3 \nu_i \mathbf{e}_i \otimes \mathbf{e}_i \in \mathbb{R}_{sym}^{3 \times 3} \mid (\mathbf{e}_1, \mathbf{e}_2, \mathbf{e}_3) \in V(\boldsymbol{\sigma}); a \geq \nu_1 \geq \nu_2 \geq \nu_3 \geq -b; \right. \\ \left. \sum_{i=1}^3 \nu_i = a - b; (\nu_1 - a)[\omega_1(\boldsymbol{\sigma}) - \omega_2(\boldsymbol{\sigma})] = 0; (\nu_3 + b)[\omega_2(\boldsymbol{\sigma}) - \omega_3(\boldsymbol{\sigma})] = 0 \right\}. \quad (2.17)$$

Conversely, one can easily check that any element from the set on the right hand side in (2.17) belongs to $\partial g(\boldsymbol{\sigma})$ using (2.5) and (2.10). \square

Remark 2.1. It is readily seen that one can specify assumptions on ν_1, ν_2 and ν_3 in (2.4) depending on $\boldsymbol{\sigma}$. For example, if $\sigma_1 > \sigma_2 > \sigma_3$ then $\nu_1 = a, \nu_2 = 0$ and $\nu_3 = -b$. The specified assumptions on ν_1, ν_2 and ν_3 will be introduced in Section 4.2.

2.2 Eigenprojections and their derivatives

It is useful to summarize some properties of eigenprojections and their derivatives, see, e.g., [19, 1]. We work with Fréchet derivatives defined in $\mathbb{R}_{sym}^{3 \times 3}$ and emphasize that some of them cannot be extended on $\mathbb{R}^{3 \times 3}$. The Fréchet derivative of function $F : \mathbb{R}_{sym}^{3 \times 3} \rightarrow \mathbb{R}$ at $\boldsymbol{\varepsilon}$ is denoted as $\mathcal{D}F(\boldsymbol{\varepsilon})$. Analogous notation, $\mathcal{D}\mathbf{F}(\boldsymbol{\varepsilon})$, is also used for tensor-valued function $\mathbf{F} : \mathbb{R}_{sym}^{3 \times 3} \rightarrow \mathbb{R}_{sym}^{3 \times 3}$. Within this subsection, the tensor variable is denoted as $\boldsymbol{\varepsilon}$ (unlike to Subsection 2.1) to be in accordance with Section 5.

Recall the spectral decomposition of $\boldsymbol{\varepsilon} \in \mathbb{R}_{sym}^{3 \times 3}$:

$$\boldsymbol{\varepsilon} = \sum_{i=1}^3 \varepsilon_i \mathbf{e}_i \otimes \mathbf{e}_i, \quad \varepsilon_1 \geq \varepsilon_2 \geq \varepsilon_3, \quad (\mathbf{e}_1, \mathbf{e}_2, \mathbf{e}_3) \in V(\boldsymbol{\varepsilon}), \quad \varepsilon_i = \omega_i(\boldsymbol{\varepsilon}), \quad i = 1, 2, 3.$$

With respect to the branching introduced in Section 5, we distinguish the following cases.

Case 1. Let $\varepsilon_1 > \varepsilon_2 > \varepsilon_3$. Then one can introduce the eigenprojections of $\mathbf{E}_i := \mathbf{E}_i(\boldsymbol{\varepsilon})$, $i = 1, 2, 3$, of $\boldsymbol{\varepsilon}$ as it follows:

$$\mathbf{E}_i = \mathbf{e}_i \otimes \mathbf{e}_i = \frac{(\boldsymbol{\varepsilon} - \varepsilon_j \mathbf{I})(\boldsymbol{\varepsilon} - \varepsilon_k \mathbf{I})}{(\varepsilon_i - \varepsilon_j)(\varepsilon_i - \varepsilon_k)}, \quad i \neq j \neq k \neq i, \quad i = 1, 2, 3. \quad (2.18)$$

Hence, $\boldsymbol{\varepsilon} = \sum_{i=1}^3 \varepsilon_i \mathbf{E}_i$ and $\sum_{i=1}^3 \mathbf{E}_i = \mathbf{I}$. Further, it is well-known that

$$\mathcal{D}\omega_i(\boldsymbol{\varepsilon}) = \mathbf{E}_i(\boldsymbol{\varepsilon}), \quad i = 1, 2, 3, \quad (2.19)$$

$$\mathcal{D}\mathbf{E}_i(\boldsymbol{\varepsilon}) = \frac{\mathcal{D}(\boldsymbol{\varepsilon}^2) - (\varepsilon_j + \varepsilon_k)\mathbb{I} - (2\varepsilon_i - \varepsilon_j - \varepsilon_k)\mathbf{E}_i \otimes \mathbf{E}_i - (\varepsilon_j - \varepsilon_k)[\mathbf{E}_j \otimes \mathbf{E}_j - \mathbf{E}_k \otimes \mathbf{E}_k]}{(\varepsilon_i - \varepsilon_j)(\varepsilon_i - \varepsilon_k)}, \quad (2.20)$$

for any $i = 1, 2, 3, i \neq j \neq k \neq i$, where the components of the fourth order tensors $\mathcal{D}(\boldsymbol{\varepsilon}^2)$ and \mathbb{I} are defined as it follows: $[\mathcal{D}(\boldsymbol{\varepsilon}^2)]_{ijkl} = \delta_{ik}[\boldsymbol{\varepsilon}]_{lj} + \delta_{jl}[\boldsymbol{\varepsilon}]_{ik}$, and $[\mathbb{I}]_{ijkl} = \delta_{ik}\delta_{jl}$, respectively¹. We use the notation $\mathbb{E}_i(\boldsymbol{\varepsilon}) := \mathcal{D}\mathbf{E}_i(\boldsymbol{\varepsilon})$, $i = 1, 2, 3$.

Case 2. Let $\varepsilon_1 \geq \varepsilon_2 > \varepsilon_3$. From (2.18), it is readily seen that the function \mathbf{E}_3 can be continuously extended for $\boldsymbol{\varepsilon}$ satisfying $\varepsilon_1 = \varepsilon_2$ unlike to \mathbf{E}_1 and \mathbf{E}_2 . Similarly, the eigenvalue functions ω_1 and ω_2 need not be differentiable at such $\boldsymbol{\varepsilon}$. On the other hand, the functions $\omega_{sum(1,2)}(\boldsymbol{\varepsilon}) := \omega_1(\boldsymbol{\varepsilon}) + \omega_2(\boldsymbol{\varepsilon})$ and $\omega_3(\boldsymbol{\varepsilon})$ are differentiable and from (2.19), one can derive:

$$\mathcal{D}\omega_3(\boldsymbol{\varepsilon}) = \mathbf{E}_3(\boldsymbol{\varepsilon}), \quad \mathcal{D}\omega_{sum(1,2)}(\boldsymbol{\varepsilon}) = \mathbf{I} - \mathbf{E}_3(\boldsymbol{\varepsilon}) =: \mathbf{E}_{12}(\boldsymbol{\varepsilon}). \quad (2.21)$$

To continuously extend function $\mathbb{E}_3(\boldsymbol{\varepsilon}) := \mathcal{D}\mathbf{E}_3(\boldsymbol{\varepsilon}) = -\mathcal{D}\mathbf{E}_{12}(\boldsymbol{\varepsilon})$ we use the equality

$$(\varepsilon_1 - \varepsilon_2)(\mathbf{E}_1 \otimes \mathbf{E}_1 - \mathbf{E}_2 \otimes \mathbf{E}_2) = (\boldsymbol{\varepsilon} - \varepsilon_3 \mathbf{E}_3) \otimes \mathbf{E}_{12} + \mathbf{E}_{12} \otimes (\boldsymbol{\varepsilon} - \varepsilon_3 \mathbf{E}_3) - (\varepsilon_1 + \varepsilon_2)\mathbf{E}_{12} \otimes \mathbf{E}_{12}$$

¹In [1, Appendix A], instead of $\mathcal{D}(\boldsymbol{\varepsilon}^2)$ and \mathbb{I} , their symmetric parts are introduced. For example, instead of \mathbb{I} , the tensor \mathbb{I}_S with the components $[\mathbb{I}_S]_{ijkl} = \frac{1}{2}(\delta_{ik}\delta_{jl} + \delta_{il}\delta_{jk})$ is considered. One can easily check that $\mathbb{I} : \boldsymbol{\varepsilon} = \mathbb{I}_S : \boldsymbol{\varepsilon} = \boldsymbol{\varepsilon}$ for any $\boldsymbol{\varepsilon} \in \mathbb{R}_{sym}^{3 \times 3}$. A similar identity also holds for $\mathcal{D}(\boldsymbol{\varepsilon}^2)$.

and substitute it into (2.20) for $i = 3$. We obtain

$$\begin{aligned} \mathbb{E}_3(\boldsymbol{\varepsilon}) &= \frac{\mathcal{D}(\boldsymbol{\varepsilon}^2) - (\varepsilon_1 + \varepsilon_2)\mathbb{I} - [\boldsymbol{\varepsilon} \otimes \mathbf{E}_{12} + \mathbf{E}_{12} \otimes \boldsymbol{\varepsilon}] + (\varepsilon_1 + \varepsilon_2)\mathbf{E}_{12} \otimes \mathbf{E}_{12}}{(\varepsilon_3 - \varepsilon_1)(\varepsilon_3 - \varepsilon_2)} + \\ &+ \frac{(\varepsilon_1 + \varepsilon_2 - 2\varepsilon_3)\mathbf{E}_3 \otimes \mathbf{E}_3 + \varepsilon_3[\mathbf{E}_{12} \otimes \mathbf{E}_3 + \mathbf{E}_3 \otimes \mathbf{E}_{12}]}{(\varepsilon_3 - \varepsilon_1)(\varepsilon_3 - \varepsilon_2)}. \end{aligned} \quad (2.22)$$

Clearly, (2.22) is well-defined also for $\varepsilon_1 = \varepsilon_2$. Notice that if $\varepsilon_1 = \varepsilon_2 > \varepsilon_3$ then $\boldsymbol{\varepsilon}$ has only two eigenprojections: \mathbf{E}_{12} and \mathbf{E}_3 , and $\boldsymbol{\varepsilon} = \varepsilon_1\mathbf{E}_{12} + \varepsilon_3\mathbf{E}_3$. Conversely, if $\varepsilon_1 > \varepsilon_2 > \varepsilon_3$, then $\mathbf{E}_{12} = \mathbf{E}_1 + \mathbf{E}_2$.

Case 3. Let $\varepsilon_1 > \varepsilon_2 \geq \varepsilon_3$. Similarly as in Case 2, the functions $\omega_1(\boldsymbol{\varepsilon})$, $\omega_{sum(2,3)}(\boldsymbol{\varepsilon}) := \omega_2(\boldsymbol{\varepsilon}) + \omega_3(\boldsymbol{\varepsilon})$ are differentiable and we have

$$\mathcal{D}\omega_1(\boldsymbol{\varepsilon}) = \mathbf{E}_1(\boldsymbol{\varepsilon}), \quad \mathcal{D}\omega_{sum(2,3)}(\boldsymbol{\varepsilon}) = \mathbf{I} - \mathbf{E}_1(\boldsymbol{\varepsilon}) =: \mathbf{E}_{23}(\boldsymbol{\varepsilon}), \quad (2.23)$$

$$\begin{aligned} \mathbb{E}_1(\boldsymbol{\varepsilon}) = \mathcal{D}\mathbf{E}_1(\boldsymbol{\varepsilon}) &= \frac{\mathcal{D}(\boldsymbol{\varepsilon}^2) - (\varepsilon_2 + \varepsilon_3)\mathbb{I} - [\boldsymbol{\varepsilon} \otimes \mathbf{E}_{23} + \mathbf{E}_{23} \otimes \boldsymbol{\varepsilon}] + (\varepsilon_2 + \varepsilon_3)\mathbf{E}_{23} \otimes \mathbf{E}_{23}}{(\varepsilon_1 - \varepsilon_2)(\varepsilon_1 - \varepsilon_3)} + \\ &+ \frac{(\varepsilon_2 + \varepsilon_3 - 2\varepsilon_1)\mathbf{E}_1 \otimes \mathbf{E}_1 + \varepsilon_1[\mathbf{E}_{23} \otimes \mathbf{E}_1 + \mathbf{E}_1 \otimes \mathbf{E}_{23}]}{(\varepsilon_1 - \varepsilon_2)(\varepsilon_1 - \varepsilon_3)}. \end{aligned} \quad (2.24)$$

Notice that if $\varepsilon_1 > \varepsilon_2 = \varepsilon_3$ then $\boldsymbol{\varepsilon}$ has only two eigenprojections: \mathbf{E}_1 and \mathbf{E}_{23} , and $\boldsymbol{\varepsilon} = \varepsilon_1\mathbf{E}_1 + \varepsilon_3\mathbf{E}_{23}$. Conversely, if $\varepsilon_1 > \varepsilon_2 > \varepsilon_3$, then $\mathbf{E}_{23} = \mathbf{E}_2 + \mathbf{E}_3$.

Case 4. Let $\varepsilon_1 \geq \varepsilon_2 \geq \varepsilon_3$. Within this general case, $\varepsilon_1 + \varepsilon_2 + \varepsilon_3 = \boldsymbol{\varepsilon} : \mathbf{I}$ and thus

$$\mathcal{D}[\omega_1 + \omega_2 + \omega_3](\boldsymbol{\varepsilon}) = \mathbf{I}. \quad (2.25)$$

Notice that if $\varepsilon_1 = \varepsilon_2 = \varepsilon_3$ then $\boldsymbol{\varepsilon} = \varepsilon_1\mathbf{I}$ and thus has only one eigenprojection: \mathbf{I} .

Remark 2.2. Eigenprojections and their derivatives can be found in simpler forms when plane strain assumptions are considered, see Appendix A.

3 The Mohr-Coulomb constitutive initial value problem

We consider the elastoplastic constitutive initial value problem containing the Mohr-Coulomb criterion, a nonassociative plastic flow rule, and a nonlinear isotropic hardening [1]:

Given the history of the strain tensor $\boldsymbol{\varepsilon} = \boldsymbol{\varepsilon}(t)$, $t \in [t_0, t_{\max}]$, and the initial values $\boldsymbol{\varepsilon}^p(t_0) = \boldsymbol{\varepsilon}^p$, $\bar{\boldsymbol{\varepsilon}}^p(t_0) = \bar{\boldsymbol{\varepsilon}}^p$. Find $(\boldsymbol{\sigma}(t), \boldsymbol{\varepsilon}^p(t), \bar{\boldsymbol{\varepsilon}}^p(t))$ such that

$$\left. \begin{aligned} \boldsymbol{\sigma} &= \mathbb{D}_e : (\boldsymbol{\varepsilon} - \boldsymbol{\varepsilon}^p), \quad \kappa = H(\bar{\boldsymbol{\varepsilon}}^p), \\ \dot{\boldsymbol{\varepsilon}}^p &\in \lambda \partial g(\boldsymbol{\sigma}), \quad \dot{\bar{\boldsymbol{\varepsilon}}^p} = -\lambda \frac{\partial f(\boldsymbol{\sigma}, \kappa)}{\partial \kappa}, \\ \dot{\lambda} &\geq 0, \quad f(\boldsymbol{\sigma}, \kappa) \leq 0, \quad \dot{\lambda} f(\boldsymbol{\sigma}, \kappa) = 0. \end{aligned} \right\} \quad (3.1)$$

hold for each instant $t \in [t_0, t_{\max}]$.

Here, $\boldsymbol{\sigma}$, $\boldsymbol{\varepsilon}^p$, $\bar{\boldsymbol{\varepsilon}}^p$, λ denote the Cauchy stress tensor, the plastic strain, the hardening variable, and the plastic multiplier, respectively. The dot symbol standardly means the pseudo-time derivative of a quantity. The functions f and g represent the yield function and the plastic pseudo-potential for the Mohr-Coulomb model, respectively:

$$f(\boldsymbol{\sigma}, \kappa) = (1 + \sin \phi)\omega_1(\boldsymbol{\sigma}) - (1 - \sin \phi)\omega_3(\boldsymbol{\sigma}) - 2(c_0 + \kappa) \cos \phi, \quad (3.2)$$

$$g(\boldsymbol{\sigma}) = (1 + \sin \psi)\omega_1(\boldsymbol{\sigma}) - (1 - \sin \psi)\omega_3(\boldsymbol{\sigma}). \quad (3.3)$$

Here, the following spectral decomposition of $\boldsymbol{\sigma}$ with the ordered principal stresses is considered:

$$\boldsymbol{\sigma} = \sum_{i=1}^3 \sigma_i \mathbf{e}_i \otimes \mathbf{e}_i, \quad \sigma_1 \geq \sigma_2 \geq \sigma_3, \quad (\mathbf{e}_1, \mathbf{e}_2, \mathbf{e}_3) \in V(\boldsymbol{\sigma}), \quad \sigma_i := \omega_i(\boldsymbol{\sigma}), \quad i = 1, 2, 3. \quad (3.4)$$

The material parameters $c_0 > 0$, $\phi, \psi \in (0, \pi/2)$ represent the initial cohesion, the friction angle, and the dilatancy angle, respectively. Notice that f, g are convex functions with respect to the stress variable. The subdifferential of g follows from Section 2.1 for the choice

$$a := 1 + \sin \psi, \quad b := 1 - \sin \psi, \quad a - b = 2 \sin \psi. \quad (3.5)$$

Clearly, $\partial f(\boldsymbol{\sigma}, \kappa)/\partial \kappa = -2 \cos \phi$.

Further, the fourth order tensor \mathbb{D}_e represents linear isotropic elastic law:

$$\boldsymbol{\sigma} = \mathbb{D}_e : \boldsymbol{\varepsilon}^e = \frac{1}{3}(3K - 2G)(\mathbf{I} : \boldsymbol{\varepsilon}^e)\mathbf{I} + 2G\boldsymbol{\varepsilon}^e, \quad \mathbb{D}_e = \frac{1}{3}(3K - 2G)\mathbf{I} \otimes \mathbf{I} + 2G\mathbb{I}, \quad (3.6)$$

where $\boldsymbol{\varepsilon}^e = \boldsymbol{\varepsilon} - \boldsymbol{\varepsilon}^p$ is the elastic part of the strain tensor and $K, G > 0$ denotes the bulk, and shear moduli, respectively.

Finally, we let the function H representing the non-linear isotropic hardening in an abstract form and assume that it is a nondecreasing, continuous, and semismooth function satisfying $H(0) = 0$.

4 Incremental constitutive problem and its solution

4.1 Implicit Euler discretization

Consider the following partition of the pseudo-time interval:

$$0 = t_0 < t_1 < \dots < t_k < \dots < t_N = t_{\max}.$$

Since we will work only with a fixed step k , we omit the index k and write $\boldsymbol{\sigma} := \boldsymbol{\sigma}(t_k)$, $\boldsymbol{\varepsilon} := \boldsymbol{\varepsilon}(t_k)$, $\boldsymbol{\varepsilon}^p := \boldsymbol{\varepsilon}^p(t_k)$ and $\bar{\boldsymbol{\varepsilon}}^p := \bar{\boldsymbol{\varepsilon}}^p(t_k)$ for the sake of simplicity. To introduce the implicit Euler discretization of the problem, we define the following trial variables: $\bar{\boldsymbol{\varepsilon}}^{p, tr} := \bar{\boldsymbol{\varepsilon}}^p(t_{k-1})$, $\boldsymbol{\varepsilon}^{tr} := \boldsymbol{\varepsilon}(t_k) - \boldsymbol{\varepsilon}^p(t_{k-1})$ and $\boldsymbol{\sigma}^{tr} := \mathbb{D}_e : \boldsymbol{\varepsilon}^{tr}$. Then the discrete elastoplastic constitutive problem for the k -step reads as it follows:

Given $\boldsymbol{\sigma}^{tr}$ and $\bar{\boldsymbol{\varepsilon}}^{p, tr}$. Find $\boldsymbol{\sigma}$, $\bar{\boldsymbol{\varepsilon}}^p$, and $\Delta\lambda$ satisfying:

$$\boldsymbol{\sigma} = \boldsymbol{\sigma}^{tr} - \Delta\lambda \mathbb{D}_e : \boldsymbol{\nu}, \quad \boldsymbol{\nu} \in \partial g(\boldsymbol{\sigma}), \quad (4.1)$$

$$\bar{\boldsymbol{\varepsilon}}^p = \bar{\boldsymbol{\varepsilon}}^{p, tr} + \Delta\lambda(2 \cos \phi), \quad (4.2)$$

$$\Delta\lambda \geq 0, \quad f(\boldsymbol{\sigma}, H(\bar{\boldsymbol{\varepsilon}}^p)) \leq 0, \quad \Delta\lambda f(\boldsymbol{\sigma}, H(\bar{\boldsymbol{\varepsilon}}^p)) = 0. \quad (4.3)$$

Notice that if problem (4.1)–(4.3) has a solution then one can set $\boldsymbol{\varepsilon}^p(t_k) = \boldsymbol{\varepsilon}(t_k) - \mathbb{D}_e^{-1} : \boldsymbol{\sigma}(t_k)$ as an input parameter for the next step.

We solve problem (4.1)–(4.3) standardly using the elastic predictor - plastic corrector method. Within the elastic prediction, we check whether

$$f(\boldsymbol{\sigma}^{tr}, H(\bar{\boldsymbol{\varepsilon}}^{p, tr})) \leq 0 \quad (4.4)$$

holds or not. If (4.4) is true, i.e., if the trial generalized stress $(\boldsymbol{\sigma}^{tr}, H(\bar{\boldsymbol{\varepsilon}}^{p, tr}))$ is admissible, then

$$\boldsymbol{\sigma} = \boldsymbol{\sigma}^{tr}, \quad \bar{\boldsymbol{\varepsilon}}^p = \bar{\boldsymbol{\varepsilon}}^{p, tr}, \quad \Delta\lambda = 0 \quad (4.5)$$

solves (4.1)–(4.3). Otherwise, it is necessary to apply the plastic correction.

4.2 Solution of the plastic correction problem

Assume that system (4.1)–(4.3) has a solution $(\boldsymbol{\sigma}, \bar{\varepsilon}^p, \Delta\lambda)$ and $f(\boldsymbol{\sigma}^{tr}, H(\bar{\varepsilon}^{p,tr})) > 0$. Then, clearly, $\Delta\lambda$ must be positive and (4.3) reduces to the equation

$$f(\boldsymbol{\sigma}, H(\bar{\varepsilon}^p)) = (1 + \sin \phi)\sigma_1 - (1 - \sin \phi)\sigma_3 - 2(c_0 + H(\bar{\varepsilon}^p)) \cos \phi = 0, \quad (4.6)$$

with respect to the spectral decomposition (3.4) of $\boldsymbol{\sigma}$. Using Lemma 2.1 and (3.5), one can choose $(\mathbf{e}_1, \mathbf{e}_2, \mathbf{e}_3) \in V(\boldsymbol{\sigma})$ such that $\boldsymbol{\nu} = \sum_{i=1}^3 \nu_i \mathbf{e}_i \otimes \mathbf{e}_i$ and

$$\left. \begin{aligned} 1 + \sin \psi \geq \nu_1 \geq \nu_2 \geq \nu_3 \geq -1 + \sin \psi, \quad \nu_1 + \nu_2 + \nu_3 = 2 \sin \psi, \\ (\nu_1 - 1 - \sin \psi)(\sigma_1 - \sigma_2) = 0, \quad (\nu_3 + 1 - \sin \psi)(\sigma_2 - \sigma_3) = 0. \end{aligned} \right\} \quad (4.7)$$

Since $\mathbf{I} = \sum_{i=1}^3 \mathbf{e}_i \otimes \mathbf{e}_i$, (3.6) implies

$$\mathbb{D}_e : \boldsymbol{\nu} = \sum_{i=1}^3 \left[\frac{2}{3}(3K - 2G) \sin \psi + 2G\nu_i \right] \mathbf{e}_i \otimes \mathbf{e}_i. \quad (4.8)$$

After the substitution of (3.4) and (4.8)₂ into (4.1), we have

$$\boldsymbol{\sigma}^{tr} = \sum_{i=1}^3 \sigma_i^{tr} \mathbf{e}_i \otimes \mathbf{e}_i, \quad \sigma_i^{tr} = \sigma_i + \Delta\lambda \left[\frac{2}{3}(3K - 2G) \sin \psi + 2G\nu_i \right], \quad i = 1, 2, 3. \quad (4.9)$$

Notice that (4.9)₁ defines the spectral decomposition of $\boldsymbol{\sigma}^{tr}$ and thus $(\mathbf{e}_1, \mathbf{e}_2, \mathbf{e}_3) \in V(\boldsymbol{\sigma}^{tr})$. Since $\sigma_1 \geq \sigma_2 \geq \sigma_3$ and $\nu_1 \geq \nu_2 \geq \nu_3$, we have:

$$(i) \quad \sigma_1^{tr} \geq \sigma_2^{tr} \geq \sigma_3^{tr};$$

$$(ii) \quad \text{if } \sigma_i^{tr} = \sigma_j^{tr} \text{ then } \sigma_i = \sigma_j, \nu_i = \nu_j.$$

From (i), it follows that the eigenvalues $\sigma_i^{tr} = \omega_i(\boldsymbol{\sigma}^{tr})$ are ordered and thus a priori known. Using (ii), one can derive that $\boldsymbol{\sigma} = \sum_{i=1}^3 \sigma_i \mathbf{e}_i^{tr} \otimes \mathbf{e}_i^{tr}$ for any $(\mathbf{e}_1^{tr}, \mathbf{e}_2^{tr}, \mathbf{e}_3^{tr}) \in V(\boldsymbol{\sigma}^{tr})$. The following lemma summarizes the proven results.

Lemma 4.1. *Let $(\boldsymbol{\sigma}, \bar{\varepsilon}^p, \Delta\lambda)$, $\Delta\lambda > 0$ be a solution to the system (4.1), (4.2), (4.6) for given $\boldsymbol{\sigma}^{tr}$ and $\bar{\varepsilon}^{p,tr}$. Let σ_i, σ_i^{tr} , $i = 1, 2, 3$, be the ordered eigenvalues of $\boldsymbol{\sigma}$, and $\boldsymbol{\sigma}^{tr}$, respectively. Then $(\sigma_1, \sigma_2, \sigma_3, \bar{\varepsilon}^p, \Delta\lambda)$ is a solution to:*

$$\sigma_i = \sigma_i^{tr} - \Delta\lambda \left[\frac{2}{3}(3K - 2G) \sin \psi + 2G\nu_i \right], \quad i = 1, 2, 3, \quad (4.10)$$

$$\bar{\varepsilon}^p = \bar{\varepsilon}^{p,tr} + \Delta\lambda(2 \cos \phi), \quad (4.11)$$

$$(1 + \sin \phi)\sigma_1 - (1 - \sin \phi)\sigma_3 - 2(c_0 + H(\bar{\varepsilon}^p)) \cos \phi = 0, \quad (4.12)$$

where ν_1, ν_2, ν_3 satisfy (4.7).

Conversely, if $(\sigma_1, \sigma_2, \sigma_3, \bar{\varepsilon}^p, \Delta\lambda)$, $\Delta\lambda > 0$ is a solution to (4.10)–(4.12) then $(\boldsymbol{\sigma}, \bar{\varepsilon}^p, \Delta\lambda)$ solves (4.1), (4.2), (4.6), where $\boldsymbol{\sigma} = \sum_{i=1}^3 \sigma_i \mathbf{e}_i \otimes \mathbf{e}_i$, $(\mathbf{e}_1, \mathbf{e}_2, \mathbf{e}_3) \in V(\boldsymbol{\sigma}^{tr})$.

To eliminate ν_1, ν_2, ν_3 from the system (4.10)–(4.12), we standardly distinguish four types of the return on the yield surface: the return to the smooth portion, the return to the left edge, the return to the right edge and the return to the apex. Within the below introduced notation, we will use: the subscripts s, l, r and a to distinguish the type of the return; the superscript “ tr ” to emphasize a known quantity depending only on the trial variables.

The return to the smooth portion. Assume $\sigma_1 > \sigma_2 > \sigma_3$. Then $\nu_1 = 1 + \sin \psi$, $\nu_2 = 0$, $\nu_3 = -(1 - \sin \psi)$ using (4.7). After substitution to (4.10), we obtain

$$\sigma_1 = \sigma_1^{tr} - \Delta\lambda \left[\frac{2}{3}(3K - 2G) \sin \psi + 2G(1 + \sin \psi) \right], \quad (4.13)$$

$$\sigma_2 = \sigma_2^{tr} - \Delta\lambda \left[\frac{2}{3}(3K - 2G) \sin \psi \right], \quad (4.14)$$

$$\sigma_3 = \sigma_3^{tr} - \Delta\lambda \left[\frac{2}{3}(3K - 2G) \sin \psi - 2G(1 - \sin \psi) \right]. \quad (4.15)$$

From (4.13)-(4.15) one can derive that $\sigma_1^{tr} > \sigma_2^{tr} > \sigma_3^{tr}$ and $0 < \Delta\lambda < \min\{\gamma_{s,l}^{tr}, \gamma_{s,r}^{tr}\}$, where

$$\gamma_{s,l}^{tr} := \frac{\sigma_1^{tr} - \sigma_2^{tr}}{2G(1 + \sin \psi)} \geq 0, \quad \gamma_{s,r}^{tr} := \frac{\sigma_2^{tr} - \sigma_3^{tr}}{2G(1 - \sin \psi)} \geq 0. \quad (4.16)$$

Define the admissible set of multipliers for this case:

$$C_s^{tr} := \{\gamma \in (0, +\infty) \mid \gamma < \min\{\gamma_{s,l}^{tr}, \gamma_{s,r}^{tr}\}\}.$$

The return to the left edge. Assume $\sigma_1 = \sigma_2 > \sigma_3$. Then $\nu_3 = -(1 - \sin \psi)$, $\nu_1 + \nu_2 = 1 + \sin \psi$, $1 + \sin \psi \geq \nu_1 \geq \nu_2 \geq 0$ using (4.7), and thus $\nu_1 - \nu_2 \leq 1 + \sin \psi$. Consequently, (4.10) yields:

$$\frac{1}{2}(\sigma_1 + \sigma_2) = \sigma_1 = \frac{1}{2}(\sigma_1^{tr} + \sigma_2^{tr}) - \Delta\lambda \left[\frac{2}{3}(3K - 2G) \sin \psi + G(1 + \sin \psi) \right], \quad (4.17)$$

$$\sigma_3 = \sigma_3^{tr} - \Delta\lambda \left[\frac{2}{3}(3K - 2G) \sin \psi - 2G(1 - \sin \psi) \right], \quad (4.18)$$

and

$$0 = \sigma_1 - \sigma_2 = \sigma_1^{tr} - \sigma_2^{tr} - \Delta\lambda[2G(\nu_1 - \nu_2)] \geq \sigma_1^{tr} - \sigma_2^{tr} - \Delta\lambda[2G(1 + \sin \psi)]. \quad (4.19)$$

From (4.17)-(4.19), it follows that $\sigma_1^{tr} \geq \sigma_2^{tr} > \sigma_3^{tr}$ and $\gamma_{s,l}^{tr} \leq \Delta\lambda < \gamma_{l,a}^{tr} < \gamma_{s,r}^{tr}$, where $\gamma_{s,l}^{tr}, \gamma_{s,r}^{tr}$ are the same as in (4.16) and

$$\gamma_{l,a}^{tr} = \frac{\sigma_1^{tr} + \sigma_2^{tr} - 2\sigma_3^{tr}}{2G(3 - \sin \psi)} = \frac{1 + \sin \psi}{3 - \sin \psi} \gamma_{s,l}^{tr} + \left(1 - \frac{1 + \sin \psi}{3 - \sin \psi}\right) \gamma_{s,r}^{tr} \geq 0. \quad (4.20)$$

Define the admissible set of multipliers for this case:

$$C_l^{tr} := \{\gamma \in (0, +\infty) \mid \gamma_{s,l}^{tr} \leq \gamma < \gamma_{l,a}^{tr}\}.$$

The return to the right edge. Assume $\sigma_1 > \sigma_2 = \sigma_3$. Then $\nu_1 = 1 + \sin \psi$, $\nu_2 + \nu_3 = -1 + \sin \psi$, $0 \geq \nu_2 \geq \nu_3 \geq -1 + \sin \psi$ using (4.7), and thus $\nu_2 - \nu_3 \leq 1 - \sin \psi$. Consequently, (4.10) yields:

$$\sigma_1 = \sigma_1^{tr} - \Delta\lambda \left[\frac{2}{3}(3K - 2G) \sin \psi + 2G(1 + \sin \psi) \right], \quad (4.21)$$

$$\frac{1}{2}(\sigma_2 + \sigma_3) = \sigma_3 = \frac{1}{2}(\sigma_2^{tr} + \sigma_3^{tr}) - \Delta\lambda \left[\frac{2}{3}(3K - 2G) \sin \psi - G(1 - \sin \psi) \right]. \quad (4.22)$$

and

$$0 = \sigma_2 - \sigma_3 = \sigma_2^{tr} - \sigma_3^{tr} - \Delta\lambda[2G(\nu_2 - \nu_3)] \geq \sigma_2^{tr} - \sigma_3^{tr} - \Delta\lambda[2G(1 - \sin \psi)]. \quad (4.23)$$

From (4.21)-(4.23), it follows that $\sigma_1^{tr} > \sigma_2^{tr} \geq \sigma_3^{tr}$ and $\gamma_{s,r}^{tr} \leq \Delta\lambda < \gamma_{r,a}^{tr} < \gamma_{s,l}^{tr}$, where $\gamma_{s,l}^{tr}, \gamma_{s,r}^{tr}$ are the same as in (4.16) and

$$\gamma_{r,a}^{tr} = \frac{2\sigma_1^{tr} - \sigma_2^{tr} - \sigma_3^{tr}}{2G(3 + \sin \psi)} = \frac{1 - \sin \psi}{3 + \sin \psi} \gamma_{s,r}^{tr} + \left(1 - \frac{1 - \sin \psi}{3 + \sin \psi}\right) \gamma_{s,l}^{tr} \geq 0. \quad (4.24)$$

Define the admissible set of multipliers for this case:

$$C_r^{tr} := \{\gamma \in (0, +\infty) \mid \gamma_{s,r}^{tr} \leq \gamma < \gamma_{r,a}^{tr}\}.$$

The return to the apex. Assume $\sigma_1 = \sigma_2 = \sigma_3$. Then $1 + \sin \psi \geq \nu_1 \geq \nu_2 \geq \nu_3 \geq -1 + \sin \psi$, $\nu_1 + \nu_2 + \nu_3 = 2 \sin \psi$ and thus $2\nu_1 - \nu_2 - \nu_3 \leq 3 + \sin \psi$, $\nu_1 + \nu_2 - 2\nu_3 \leq 3 - \sin \psi$. Consequently, (4.10) yields:

$$\sigma_1 = \frac{1}{3}(\sigma_1 + \sigma_2 + \sigma_3) = \frac{1}{3}(\sigma_1^{tr} + \sigma_2^{tr} + \sigma_3^{tr}) - \Delta\lambda[2K \sin \psi] \quad (4.25)$$

and

$$0 = 2\sigma_1 - \sigma_2 - \sigma_3 \geq 2\sigma_1^{tr} - \sigma_2^{tr} - \sigma_3^{tr} - \Delta\lambda[2G(3 + \sin \psi)], \quad (4.26)$$

$$0 = \sigma_1 + \sigma_2 - 2\sigma_3 \geq \sigma_1^{tr} + \sigma_2^{tr} - 2\sigma_3^{tr} - \Delta\lambda[2G(3 - \sin \psi)]. \quad (4.27)$$

From (4.26),(4.27), we have $\Delta\lambda \geq \max\{\gamma_{l,a}^{tr}, \gamma_{r,a}^{tr}\}$ where $\gamma_{l,a}^{tr}, \gamma_{r,a}^{tr}$ are the same as in (4.20), (4.24), respectively. Define the admissible set of multipliers for this case:

$$C_a^{tr} := \{\gamma \in (0, +\infty) \mid \gamma \geq \max\{\gamma_{l,a}^{tr}, \gamma_{r,a}^{tr}\}\}.$$

Notice that the introduced nonnegative values $\gamma_{s,l}^{tr}, \gamma_{s,r}^{tr}, \gamma_{l,a}^{tr}$, and $\gamma_{r,a}^{tr}$ are known. Moreover, from (4.16), (4.20) and (4.24), it follows that only two ordering of these values are possible: Case 1: $\gamma_{s,l}^{tr} \leq \gamma_{l,a}^{tr} \leq \gamma_{r,a}^{tr} \leq \gamma_{s,r}^{tr}$; Case 2: $\gamma_{s,r}^{tr} \leq \gamma_{r,a}^{tr} \leq \gamma_{l,a}^{tr} \leq \gamma_{s,l}^{tr}$.

Case 1. Assume $\gamma_{s,l}^{tr} \leq \gamma_{s,r}^{tr}$. Then $C_s^{tr} = (0, \gamma_{s,l}^{tr})$, $C_l^{tr} = [\gamma_{s,l}^{tr}, \gamma_{l,a}^{tr})$, $C_r^{tr} = \emptyset$ and $C_a^{tr} = [\gamma_{l,a}^{tr}, +\infty)$. Hence, one can uniformly write:

$$\begin{aligned} \sigma_1 &= \sigma_1^{tr} - \Delta\lambda \left[\frac{2}{3}(3K - 2G) \sin \psi + 2G(1 + \sin \psi) \right] + \\ &\quad + G(1 + \sin \psi)(\Delta\lambda - \gamma_{s,l}^{tr})^+ + \frac{1}{3}G(3 - \sin \psi)(\Delta\lambda - \gamma_{l,a}^{tr})^+, \end{aligned} \quad (4.28)$$

$$\begin{aligned} \sigma_2 &= \sigma_2^{tr} - \Delta\lambda \left[\frac{2}{3}(3K - 2G) \sin \psi \right] - \\ &\quad - G(1 + \sin \psi)(\Delta\lambda - \gamma_{s,l}^{tr})^+ + \frac{1}{3}G(3 - \sin \psi)(\Delta\lambda - \gamma_{l,a}^{tr})^+, \end{aligned} \quad (4.29)$$

$$\begin{aligned} \sigma_3 &= \sigma_3^{tr} - \Delta\lambda \left[\frac{2}{3}(3K - 2G) \sin \psi - 2G(1 - \sin \psi) \right] - \\ &\quad - \frac{2}{3}G(3 - \sin \psi)(\Delta\lambda - \gamma_{l,a}^{tr})^+, \end{aligned} \quad (4.30)$$

where $(.)^+$ denotes a positive part of a function. For example, the equalities (4.13), (4.17), and (4.25) are included in (4.28). After substitution (4.28), (4.30), and (4.2) into (4.6), we receive $q^{tr}(\Delta\lambda) = 0$ where

$$\begin{aligned} q^{tr}(\gamma) &:= (1 + \sin \phi)\sigma_1^{tr} - (1 - \sin \phi)\sigma_3^{tr} - \gamma \left[\frac{4}{3}(3K - 2G) \sin \psi \sin \phi + 4G(1 + \sin \psi \sin \phi) \right] \\ &\quad + G(1 + \sin \psi)(1 + \sin \phi)(\gamma - \gamma_{s,l}^{tr})^+ + \frac{1}{3}G(3 - \sin \psi)(3 - \sin \phi)(\gamma - \gamma_{l,a}^{tr})^+ \\ &\quad - 2 [c_0 + H(\bar{\varepsilon}^{p,tr} + \gamma(2 \cos \phi))] \cos \phi, \quad \gamma \in (0, +\infty). \end{aligned} \quad (4.31)$$

It is readily seen that the function q is continuous on \mathbb{R}_+ . Denote q_s^{tr} , q_l^{tr} , and q_a^{tr} as the restrictions of q^{tr} on C_s^{tr} , C_l^{tr} , C_a^{tr} , respectively. It holds:

$$\begin{aligned} q_s^{tr}(\gamma) &= (1 + \sin \phi)\sigma_1^{tr} - (1 - \sin \phi)\sigma_3^{tr} - 2 [c_0 + H(\bar{\varepsilon}^{p,tr} + \gamma(2 \cos \phi))] \cos \phi \\ &\quad - \gamma \left[\frac{4}{3}(3K - 2G) \sin \psi \sin \phi + 4G(1 + \sin \psi \sin \phi) \right], \end{aligned} \quad (4.32)$$

$$\begin{aligned} q_l^{tr}(\gamma) &= \frac{1}{2}(1 + \sin \phi)(\sigma_1^{tr} + \sigma_2^{tr}) - (1 - \sin \phi)\sigma_3^{tr} - 2 [c_0 + H(\bar{\varepsilon}^{p,tr} + \gamma(2 \cos \phi))] \cos \phi - \\ &\quad \gamma \left[\frac{4}{3}(3K - 2G) \sin \psi \sin \phi + G(1 + \sin \psi)(1 + \sin \phi) + 2G(1 - \sin \psi)(1 - \sin \phi) \right], \end{aligned} \quad (4.33)$$

$$q_a^{tr}(\gamma) = \frac{2}{3}(\sigma_1^{tr} + \sigma_2^{tr} + \sigma_3^{tr}) \sin \phi - 2 [c_0 + H(\bar{\varepsilon}^{p,tr} + \gamma(2 \cos \phi))] \cos \phi - \gamma[4K \sin \psi \sin \phi]. \quad (4.34)$$

From (4.32)-(4.34), it is readily seen that the function q is decreasing and unbounded from below on \mathbb{R}_+ . Moreover,

$$q^{tr}(0) = q_s^{tr}(0) = f(\boldsymbol{\sigma}^{tr}, H(\bar{\varepsilon}^{p,tr})) > 0$$

within the plastic correction. Therefore, the unknown multiplier $\Delta\lambda$ is a unique solution to the equation $q^{tr}(\gamma) = 0$.

Case 2. Assume $\gamma_{s,r}^{tr} \leq \gamma_{s,l}^{tr}$. Then $C_s^{tr} = (0, \gamma_{s,r}^{tr})$, $C_l^{tr} = \emptyset$, $C_r^{tr} = [\gamma_{s,r}^{tr}, \gamma_{r,a}^{tr})$, and $C_a^{tr} = [\gamma_{r,a}^{tr}, +\infty)$. Hence, one can uniformly write:

$$\begin{aligned} \sigma_1 &= \sigma_1^{tr} - \Delta\lambda \left[\frac{2}{3}(3K - 2G) \sin \psi + 2G(1 + \sin \psi) \right] + \\ &\quad + \frac{2}{3}G(3 + \sin \psi)(\Delta\lambda - \gamma_{r,a}^{tr})^+, \end{aligned} \quad (4.35)$$

$$\begin{aligned} \sigma_2 &= \sigma_2^{tr} - \Delta\lambda \left[\frac{2}{3}(3K - 2G) \sin \psi \right] + \\ &\quad + \frac{1}{2}2G(1 - \sin \psi)(\Delta\lambda - \gamma_{s,r}^{tr})^+ - \frac{1}{3}G(3 + \sin \psi)(\Delta\lambda - \gamma_{r,a}^{tr})^+, \end{aligned} \quad (4.36)$$

$$\begin{aligned} \sigma_3 &= \sigma_3^{tr} - \Delta\lambda \left[\frac{2}{3}(3K - 2G) \sin \psi - 2G(1 - \sin \psi) \right] - \\ &\quad - G(1 - \sin \psi)(\Delta\lambda - \gamma_{s,r}^{tr})^+ - \frac{1}{3}G(3 + \sin \psi)(\Delta\lambda - \gamma_{r,a}^{tr})^+. \end{aligned} \quad (4.37)$$

where $(\cdot)^+$ denotes a positive part of a function. After substitution (4.35), (4.37), and (4.2) into (4.6), we receive $\hat{q}^{tr}(\Delta\lambda) = 0$ where

$$\begin{aligned} \hat{q}^{tr}(\gamma) &= (1 + \sin \phi)\sigma_1^{tr} - (1 - \sin \phi)\sigma_3^{tr} - \gamma \left[\frac{4}{3}(3K - 2G) \sin \psi \sin \phi + 4G(1 + \sin \psi \sin \phi) \right] \\ &\quad + G(1 - \sin \psi)(1 - \sin \phi)(\gamma - \gamma_{s,r}^{tr})^+ + \frac{1}{3}G(3 + \sin \psi)(3 + \sin \phi)(\gamma - \gamma_{r,a}^{tr})^+ \\ &\quad - 2 [c_0 + H(\bar{\varepsilon}^{p,tr} + \gamma(2 \cos \phi))] \cos \phi. \end{aligned} \quad (4.38)$$

It is readily seen that the function \hat{q} is continuous on \mathbb{R}_+ . Notice that $q_s^{tr} = \hat{q}|_{C_s^{tr}}$ and $q_a^{tr} = \hat{q}|_{C_a^{tr}}$. Denote $q_r^{tr} := \hat{q}|_{C_r^{tr}}$. It holds that

$$\begin{aligned} q_r^{tr}(\gamma) &= (1 + \sin \phi)\sigma_1^{tr} - \frac{1}{2}(1 - \sin \phi)(\sigma_2^{tr} + \sigma_3^{tr}) - 2 [c_0 + H(\bar{\varepsilon}^{p,tr} + \gamma(2 \cos \phi))] \cos \phi - \\ &\quad \gamma \left[\frac{4}{3}(3K - 2G) \sin \psi \sin \phi + 2G(1 + \sin \psi)(1 + \sin \phi) + G(1 - \sin \psi)(1 - \sin \phi) \right]. \end{aligned} \quad (4.39)$$

From (4.32), (4.34) and (4.39), it is readily seen that the function \hat{q} is decreasing, unbounded from below on \mathbb{R}_+ and $\hat{q}^{tr}(0) = q^{tr}(0) > 0$ within the plastic correction. Therefore, the unknown multiplier $\Delta\lambda$ is a unique solution to the equation $\hat{q}^{tr}(\gamma) = 0$.

The following theorem summarizes the proven results.

Theorem 4.1. *Let $f(\boldsymbol{\sigma}^{tr}, H(\bar{\varepsilon}^{p, tr})) > 0$, i.e., the plastic correction happen. Then problem (4.1), (4.2), (4.6) and problem (4.10)-(4.12) have unique solutions. The solution $(\sigma_1, \sigma_2, \sigma_3, \bar{\varepsilon}^p, \Delta\lambda)$ to (4.10)-(4.12) can be found in the following way.*

1. *Let $q_s^{tr}(\min\{\gamma_{s,l}^{tr}, \gamma_{s,r}^{tr}\}) < 0$. Then $\sigma_1^{tr} > \sigma_2^{tr} > \sigma_3^{tr}$, $\Delta\lambda \in C_s^{tr}$ is the unique solution to $q_s^{tr}(\Delta\lambda) = 0$ and $\sigma_1 > \sigma_2 > \sigma_3$ can be computed from (4.13)-(4.15).*
2. *Let $\gamma_{s,l}^{tr} < \gamma_{l,a}^{tr}$, $q_l^{tr}(\gamma_{s,l}^{tr}) \geq 0$ and $q_l^{tr}(\gamma_{l,a}^{tr}) < 0$. Then $\sigma_1^{tr} \geq \sigma_2^{tr} > \sigma_3^{tr}$, $\Delta\lambda \in C_l^{tr}$ is the unique solution to $q_l^{tr}(\Delta\lambda) = 0$ and $\sigma_1 = \sigma_2 > \sigma_3$ can be computed from (4.17), and (4.18). Moreover, $\Delta\lambda$, σ_1 and σ_3 depend on σ_1^{tr} and σ_2^{tr} only through $\sigma_1^{tr} + \sigma_2^{tr}$.*
3. *Let $\gamma_{s,r}^{tr} < \gamma_{r,a}^{tr}$, $q_r^{tr}(\gamma_{s,r}^{tr}) \geq 0$ and $q_r^{tr}(\gamma_{r,a}^{tr}) < 0$. Then $\sigma_1^{tr} > \sigma_2^{tr} \geq \sigma_3^{tr}$, $\Delta\lambda \in C_r^{tr}$ is the unique solution to $q_r^{tr}(\Delta\lambda) = 0$ and $\sigma_1 > \sigma_2 = \sigma_3$ can be computed from (4.21), and (4.22). Moreover, $\Delta\lambda$, σ_1 and σ_3 depend on σ_2^{tr} and σ_3^{tr} only through $\sigma_2^{tr} + \sigma_3^{tr}$.*
4. *Let $q_a^{tr}(\max\{\gamma_{l,a}^{tr}, \gamma_{r,a}^{tr}\}) \geq 0$. Then $\Delta\lambda \in C_a^{tr}$ is the unique solution to $q_a^{tr}(\Delta\lambda) = 0$ and $\sigma_1 = \sigma_2 = \sigma_3$ can be computed from (4.25). Moreover, $\Delta\lambda$ and σ_1 depend on σ_1^{tr} , σ_2^{tr} and σ_3^{tr} only through $\sigma_1^{tr} + \sigma_2^{tr} + \sigma_3^{tr}$.*

The solution component $\bar{\varepsilon}^p$ can be updated from (4.11) for all of these cases.

Remark 4.1. Theorem 4.1 summarizes the advantages of the new technique based on the subdifferential formulation of the flow rule in comparison with the current approach. First, one can a priori decide about the type of the return even if nonlinear hardening is introduced. Second, the dependence of the solution $(\sigma_1, \sigma_2, \sigma_3, \bar{\varepsilon}^p, \Delta\lambda)$ on the trial principal stresses has been more specified than it is known from literature. This enables to investigate strong semismoothness of the stress-strain operator and significantly reduce branching within construction of the consistent tangent operator, see the next section.

5 Stress-strain and consistent tangent operators

Recall that $\bar{\varepsilon}^{p, tr} = \bar{\varepsilon}^p(t_{k-1})$, $\boldsymbol{\varepsilon}^{tr} = \boldsymbol{\varepsilon}(t_k) - \boldsymbol{\varepsilon}^p(t_{k-1})$ and $\boldsymbol{\sigma}^{tr} = \mathbb{D}_e : \boldsymbol{\varepsilon}^{tr}$. Consequently, one can define the implicit function \mathbf{T} representing the above described stress-strain relation:

$$\boldsymbol{\sigma}(t_k) := \mathbf{T}(\boldsymbol{\varepsilon}(t_k); \boldsymbol{\varepsilon}^p(t_{k-1}), \bar{\varepsilon}^p(t_{k-1})) = \mathbf{S}(\boldsymbol{\varepsilon}^{tr}, \bar{\varepsilon}^{p, tr}). \quad (5.1)$$

For numerical purposes, it is more convenient to work with eigenprojections than with eigenvectors since the eigenprojections are uniquely determined. Therefore, to determine (5.1) and its derivative $\mathcal{D}_{\boldsymbol{\varepsilon}}\mathbf{T} = \mathcal{D}_{\boldsymbol{\varepsilon}^{tr}}\mathbf{S}$ (if it exists), we use the framework from Section 2.2. Here, $\mathcal{D}_{\boldsymbol{\varepsilon}^{tr}}$ denotes the Fréchet derivative of a function with respect to the variable $\boldsymbol{\varepsilon}^{tr}$. For the sake of brevity, we omit this subscript and write $\mathcal{D} \equiv \mathcal{D}_{\boldsymbol{\varepsilon}^{tr}}$ from now on. Further, it is worth mentioning that $\boldsymbol{\sigma}^{tr}$ and $\boldsymbol{\varepsilon}^{tr}$ have the same eigenvectors and eigenprojections, and it holds that

$$\sigma_i^{tr} = \frac{1}{3}(3K - 2G)(\varepsilon_1^{tr} + \varepsilon_2^{tr} + \varepsilon_3^{tr}) + 2G\varepsilon_i^{tr}, \quad i = 1, 2, 3. \quad (5.2)$$

where ε_i^{tr} , $i = 1, 2, 3$, denote the eigenvalues of $\boldsymbol{\varepsilon}^{tr}$.

Now, we introduce the operators \mathbf{S} and $\mathcal{D}\mathbf{S}$ on the open sets

$$\begin{aligned} M_e^{tr} &:= \{\boldsymbol{\varepsilon}^{tr} \in \mathbb{R}_{sym}^{3 \times 3} \mid q^{tr}(0) = \hat{q}^{tr}(0) = q_s^{tr}(0) = f(\mathbb{D}_e : \boldsymbol{\varepsilon}^{tr}, H(\bar{\varepsilon}^{p,tr})) < 0\}, \\ M_s^{tr} &:= \{\boldsymbol{\varepsilon}^{tr} \in \mathbb{R}_{sym}^{3 \times 3} \mid q_s^{tr}(0) > 0, q_s^{tr}(\min\{\gamma_{s,l}^{tr}, \gamma_{s,r}^{tr}\}) < 0\}, \\ M_l^{tr} &:= \{\boldsymbol{\varepsilon}^{tr} \in \mathbb{R}_{sym}^{3 \times 3} \mid \gamma_{s,l}^{tr} < \gamma_{l,a}^{tr}, q_l^{tr}(\gamma_{s,l}^{tr}) > 0, q_l^{tr}(\gamma_{l,a}^{tr}) < 0\}, \\ M_r^{tr} &:= \{\boldsymbol{\varepsilon}^{tr} \in \mathbb{R}_{sym}^{3 \times 3} \mid \gamma_{s,r}^{tr} < \gamma_{r,a}^{tr}, q_r^{tr}(\gamma_{s,r}^{tr}) > 0, q_r^{tr}(\gamma_{r,a}^{tr}) < 0\}, \\ M_a^{tr} &:= \{\boldsymbol{\varepsilon}^{tr} \in \mathbb{R}_{sym}^{3 \times 3} \mid q_a^{tr}(\max\{\gamma_{l,a}^{tr}, \gamma_{r,a}^{tr}\}) > 0\}. \end{aligned}$$

From Section 4, it follows that these sets are mutually disjoint and the closure of their union is equal to $\mathbb{R}_{sym}^{3 \times 3}$. For the sake of simplicity, we assume that H is differentiable at $\bar{\varepsilon}_k^{p,tr} + \Delta\lambda(2 \cos \phi)$ and denote $H_1 := H'(\bar{\varepsilon}_k^{p,tr} + \Delta\lambda(2 \cos \phi))$.

Elastic response. Let $\boldsymbol{\varepsilon}^{tr} \in M_e^{tr}$. Then, clearly,

$$\mathbf{S}(\boldsymbol{\varepsilon}^{tr}, \bar{\varepsilon}^{p,tr}) = \mathbb{D}_e : \boldsymbol{\varepsilon}^{tr}, \quad \mathcal{D}\mathbf{S}(\boldsymbol{\varepsilon}^{tr}, \bar{\varepsilon}^{p,tr}) = \mathbb{D}_e. \quad (5.3)$$

Return to the smooth portion. Let $\boldsymbol{\varepsilon}^{tr} \in M_s^{tr}$. Then $\varepsilon_1^{tr} > \varepsilon_2^{tr} > \varepsilon_3^{tr}$. It means that one can introduce the notation $\mathbf{E}_i^{tr} := \mathbf{E}_i(\boldsymbol{\varepsilon}^{tr})$, $\mathbb{E}_i^{tr} := \mathbb{E}_i(\boldsymbol{\varepsilon}^{tr})$, $i = 1, 2, 3$, and write

$$\mathbf{S}(\boldsymbol{\varepsilon}^{tr}, \bar{\varepsilon}^{p,tr}) = \sum_{i=1}^3 \sigma_i \mathbf{E}_i^{tr}, \quad \mathcal{D}\mathbf{S}(\boldsymbol{\varepsilon}^{tr}, \bar{\varepsilon}^{p,tr}) = \sum_{i=1}^3 [\sigma_i \mathbb{E}_i^{tr} + \mathbf{E}_i^{tr} \otimes \mathcal{D}\sigma_i]. \quad (5.4)$$

Since,

$$\begin{aligned} \mathcal{D}\sigma_1 &\stackrel{(4.13)}{=} \frac{1}{3}(3K - 2G)\mathbf{I} + 2G\mathbf{E}_1^{tr} - \mathcal{D}(\Delta\lambda) \left[\frac{2}{3}(3K - 2G) \sin \psi + 2G(1 + \sin \psi) \right], \\ \mathcal{D}\sigma_2 &\stackrel{(4.14)}{=} \frac{1}{3}(3K - 2G)\mathbf{I} + 2G\mathbf{E}_2^{tr} - \mathcal{D}(\Delta\lambda) \left[\frac{2}{3}(3K - 2G) \sin \psi \right], \\ \mathcal{D}\sigma_3 &\stackrel{(4.15)}{=} \frac{1}{3}(3K - 2G)\mathbf{I} + 2G\mathbf{E}_3^{tr} - \mathcal{D}(\Delta\lambda) \left[\frac{2}{3}(3K - 2G) \sin \psi - 2G(1 - \sin \psi) \right], \end{aligned}$$

we have

$$\begin{aligned} \mathcal{D}\mathbf{S}(\boldsymbol{\varepsilon}^{tr}, \bar{\varepsilon}^{p,tr}) &= \sum_{i=1}^3 [\sigma_i \mathbb{E}_i^{tr} + 2G\mathbf{E}_i^{tr} \otimes \mathbf{E}_i^{tr}] + \frac{1}{3}(3K - 2G)\mathbf{I} \otimes \mathbf{I} - \\ &\quad - \left[2G(1 + \sin \psi)\mathbf{E}_1^{tr} - 2G(1 - \sin \psi)\mathbf{E}_3^{tr} + \frac{2}{3}(3K - 2G) \sin \psi \mathbf{I} \right] \otimes \mathcal{D}(\Delta\lambda), \end{aligned} \quad (5.5)$$

where

$$\mathcal{D}(\Delta\lambda) \stackrel{(4.32)}{=} \frac{2G(1 + \sin \phi)\mathbf{E}_1^{tr} - 2G(1 - \sin \phi)\mathbf{E}_3^{tr} + \frac{2}{3}(3K - 2G) \sin \phi \mathbf{I}}{\frac{4}{3}(3K - 2G) \sin \psi \sin \phi + 4G(1 + \sin \psi \sin \phi) + 4H_1 \cos^2 \phi}.$$

Return to the left edge. Let $\boldsymbol{\varepsilon}^{tr} \in M_l^{tr}$. Then $\varepsilon_1^{tr} \geq \varepsilon_2^{tr} > \varepsilon_3^{tr}$. It means that one can introduce the notation $\mathbf{E}_3^{tr} := \mathbf{E}_3(\boldsymbol{\varepsilon}^{tr})$, $\mathbf{E}_{12}^{tr} := \mathbf{I} - \mathbf{E}_3^{tr}$, $\mathbb{E}_3^{tr} := \mathbb{E}_3(\boldsymbol{\varepsilon}^{tr})$ and write

$$\mathbf{S}(\boldsymbol{\varepsilon}^{tr}, \bar{\varepsilon}^{p,tr}) = \sigma_1 \mathbf{E}_{12}^{tr} + \sigma_3 \mathbf{E}_3^{tr}, \quad \mathcal{D}\mathbf{S}(\boldsymbol{\varepsilon}^{tr}, \bar{\varepsilon}^{p,tr}) = (\sigma_3 - \sigma_1)\mathbb{E}_3^{tr} + \mathbf{E}_{12}^{tr} \otimes \mathcal{D}\sigma_1 + \mathbf{E}_3^{tr} \otimes \mathcal{D}\sigma_3. \quad (5.6)$$

Since,

$$\begin{aligned} \mathcal{D}\sigma_1 &\stackrel{(4.17)}{=} \frac{1}{3}(3K - 2G)\mathbf{I} + G\mathbf{E}_{12}^{tr} - \mathcal{D}(\Delta\lambda) \left[\frac{2}{3}(3K - 2G) \sin \psi + G(1 + \sin \psi) \right], \\ \mathcal{D}\sigma_3 &\stackrel{(4.18)}{=} \frac{1}{3}(3K - 2G)\mathbf{I} + 2G\mathbf{E}_3^{tr} - \mathcal{D}(\Delta\lambda) \left[\frac{2}{3}(3K - 2G) \sin \psi - 2G(1 - \sin \psi) \right], \end{aligned}$$

we have

$$\begin{aligned} \mathcal{D}\mathbf{S}(\boldsymbol{\varepsilon}^{tr}, \bar{\boldsymbol{\varepsilon}}^{p,tr}) &= (\sigma_3 - \sigma_1)\mathbb{E}_3^{tr} + G\mathbf{E}_{12}^{tr} \otimes \mathbf{E}_{12}^{tr} + 2G\mathbf{E}_3^{tr} \otimes \mathbf{E}_3^{tr} + \frac{1}{3}(3K - 2G)\mathbf{I} \otimes \mathbf{I} - \\ &\quad - \left[G(1 + \sin \psi)\mathbf{E}_{12}^{tr} - 2G(1 - \sin \psi)\mathbf{E}_3^{tr} + \frac{2}{3}(3K - 2G)\sin \psi \mathbf{I} \right] \otimes \mathcal{D}(\Delta\lambda), \end{aligned} \quad (5.7)$$

where

$$\mathcal{D}(\Delta\lambda) \stackrel{(4.33)}{=} \frac{G(1 + \sin \phi)\mathbf{E}_{12}^{tr} - 2G(1 - \sin \phi)\mathbf{E}_3^{tr} + \frac{2}{3}(3K - 2G)\sin \phi \mathbf{I}}{\frac{4}{3}(3K - 2G)\sin \psi \sin \phi + G(1 + \sin \psi)(1 + \sin \phi) + 2G(1 - \sin \psi)(1 - \sin \phi) + 4H_1 \cos^2 \phi}.$$

Return to the right edge. Let $\boldsymbol{\varepsilon}^{tr} \in M_r^{tr}$. Then $\varepsilon_1^{tr} > \varepsilon_2^{tr} \geq \varepsilon_3^{tr}$. It means that one can introduce the notation $\mathbf{E}_1^{tr} := \mathbf{E}_1(\boldsymbol{\varepsilon}^{tr})$, $\mathbf{E}_{23}^{tr} := \mathbf{I} - \mathbf{E}_1^{tr}$, $\mathbb{E}_1^{tr} := \mathbb{E}_1(\boldsymbol{\varepsilon}^{tr})$ and write

$$\mathbf{S}(\boldsymbol{\varepsilon}^{tr}, \bar{\boldsymbol{\varepsilon}}^{p,tr}) = \sigma_1\mathbf{E}_1^{tr} + \sigma_3\mathbf{E}_{23}^{tr}, \quad \mathcal{D}\mathbf{S}(\boldsymbol{\varepsilon}^{tr}, \bar{\boldsymbol{\varepsilon}}^{p,tr}) = (\sigma_1 - \sigma_3)\mathbb{E}_1^{tr} + \mathbf{E}_1^{tr} \otimes \mathcal{D}\sigma_1 + \mathbf{E}_{23}^{tr} \otimes \mathcal{D}\sigma_3. \quad (5.8)$$

Since,

$$\begin{aligned} \mathcal{D}\sigma_1 &\stackrel{(4.21)}{=} \frac{1}{3}(3K - 2G)\mathbf{I} + 2G\mathbf{E}_1^{tr} - \mathcal{D}(\Delta\lambda) \left[\frac{2}{3}(3K - 2G)\sin \psi + 2G(1 + \sin \psi) \right], \\ \mathcal{D}\sigma_3 &\stackrel{(4.22)}{=} \frac{1}{3}(3K - 2G)\mathbf{I} + G\mathbf{E}_{23}^{tr} - \mathcal{D}(\Delta\lambda) \left[\frac{2}{3}(3K - 2G)\sin \psi - G(1 - \sin \psi) \right], \end{aligned}$$

we have

$$\begin{aligned} \mathcal{D}\mathbf{S}(\boldsymbol{\varepsilon}^{tr}, \bar{\boldsymbol{\varepsilon}}^{p,tr}) &= (\sigma_1 - \sigma_3)\mathbb{E}_1^{tr} + 2G\mathbf{E}_1^{tr} \otimes \mathbf{E}_1^{tr} + G\mathbf{E}_{23}^{tr} \otimes \mathbf{E}_{23}^{tr} + \frac{1}{3}(3K - 2G)\mathbf{I} \otimes \mathbf{I} - \\ &\quad - \left[2G(1 + \sin \psi)\mathbf{E}_1^{tr} - G(1 - \sin \psi)\mathbf{E}_{23}^{tr} + \frac{2}{3}(3K - 2G)\sin \psi \mathbf{I} \right] \otimes \mathcal{D}(\Delta\lambda), \end{aligned} \quad (5.9)$$

where

$$\mathcal{D}(\Delta\lambda) \stackrel{(4.39)}{=} \frac{2G(1 + \sin \phi)\mathbf{E}_1^{tr} - G(1 - \sin \phi)\mathbf{E}_{23}^{tr} + \frac{2}{3}(3K - 2G)\sin \phi \mathbf{I}}{\frac{4}{3}(3K - 2G)\sin \psi \sin \phi + 2G(1 + \sin \psi)(1 + \sin \phi) + G(1 - \sin \psi)(1 - \sin \phi) + 4H_1 \cos^2 \phi}.$$

Return to the apex. Let $\boldsymbol{\varepsilon}^{tr} \in M_a^{tr}$. Then

$$\mathbf{S}(\boldsymbol{\varepsilon}^{tr}, \bar{\boldsymbol{\varepsilon}}^{p,tr}) = p\mathbf{I}, \quad p = p^{tr} - (2K \sin \psi)\Delta\lambda, \quad p^{tr} = \frac{1}{3}(\sigma_1^{tr} + \sigma_2^{tr} + \sigma_3^{tr}) = K(\varepsilon_1^{tr} + \varepsilon_2^{tr} + \varepsilon_3^{tr}), \quad (5.10)$$

$$\mathcal{D}\mathbf{S}(\boldsymbol{\varepsilon}^{tr}, \bar{\boldsymbol{\varepsilon}}^{p,tr}) \stackrel{(5.10)}{=} \frac{\partial p}{\partial p^{tr}} K\mathbf{I} \otimes \mathbf{I} = \left(1 - 2K \sin \psi \frac{\partial \Delta\lambda}{\partial p^{tr}} \right) K\mathbf{I} \otimes \mathbf{I}.$$

Here, we use $\frac{\partial p^{tr}}{\partial \boldsymbol{\varepsilon}^{tr}} = K\mathbf{I}$. From the implicit equation $q_a^{tr}(\Delta\lambda) = 0$, we obtain

$$\frac{\partial \Delta\lambda}{\partial p^{tr}} \stackrel{(4.34)}{=} \frac{\sin \phi}{2K \sin \psi \sin \phi + 2H_1 \cos^2 \phi}.$$

Hence,

$$\mathcal{D}\mathbf{S}(\boldsymbol{\varepsilon}^{tr}, \bar{\boldsymbol{\varepsilon}}^{p,tr}) = K \left(1 - \frac{K \sin \psi \sin \phi}{K \sin \psi \sin \phi + H_1 \cos^2 \phi} \right) \mathbf{I} \otimes \mathbf{I}. \quad (5.11)$$

Notice that one can continuously extend the definition of $\mathbf{T}(\cdot; \boldsymbol{\varepsilon}^p(t_{k-1}), \bar{\boldsymbol{\varepsilon}}^p(t_{k-1})) = \mathbf{S}(\cdot, \bar{\boldsymbol{\varepsilon}}^{p, tr})$ on

$$\mathbb{R}_{sym}^{3 \times 3} \setminus (M_e^{tr} \cup M_s^{tr} \cup M_l^{tr} \cup M_r^{tr} \cup M_a^{tr}).$$

Further, one can investigate semismoothness of $\mathbf{T}(\cdot; \boldsymbol{\varepsilon}^p(t_{k-1}), \bar{\boldsymbol{\varepsilon}}^p(t_{k-1}))$ for any $\boldsymbol{\varepsilon}(t_k)$. To show the semismoothness in M_e^{tr} , M_s^{tr} , M_l^{tr} , M_r^{tr} , and M_a^{tr} , one can use the framework introduced in [2]. At the remaining points, the proof seems to be technically complicated, and we skip it for the sake of brevity. Therefore, we will only assume that $\mathbf{T}(\cdot; \boldsymbol{\varepsilon}^p(t_{k-1}), \bar{\boldsymbol{\varepsilon}}^p(t_{k-1}))$ is semismooth for any $\boldsymbol{\varepsilon}(t_k)$ to introduce the semismooth Newton method in the next section. We denote $\mathbb{T}(\cdot; \boldsymbol{\varepsilon}^p(t_{k-1}), \bar{\boldsymbol{\varepsilon}}^p(t_{k-1}))$ as the generalized derivative of $\mathbf{T}(\cdot; \boldsymbol{\varepsilon}^p(t_{k-1}), \bar{\boldsymbol{\varepsilon}}^p(t_{k-1}))$ in $\mathbb{R}_{sym}^{3 \times 3}$ in the Clark sense. Clearly, $\mathbb{T}(\boldsymbol{\varepsilon}(t_k); \boldsymbol{\varepsilon}^p(t_{k-1}), \bar{\boldsymbol{\varepsilon}}^p(t_{k-1})) = \mathcal{D}_{\boldsymbol{\varepsilon}} \mathbf{T}(\boldsymbol{\varepsilon}(t_k); \boldsymbol{\varepsilon}^p(t_{k-1}), \bar{\boldsymbol{\varepsilon}}^p(t_{k-1}))$ when $\mathbf{T}(\cdot; \boldsymbol{\varepsilon}^p(t_{k-1}), \bar{\boldsymbol{\varepsilon}}^p(t_{k-1}))$ is differentiable at $\boldsymbol{\varepsilon}(t_k)$.

6 Numerical realization of the incremental boundary value elastoplastic problem

The stress-strain operator \mathbf{T} is standardly substituted into the balance equation leading to the incremental boundary value elastoplastic problem in small strains at the k -th step [1, 2]. This problem is further discretized in space by the finite element method. For the sake of brevity, we focus only on an algebraic formulation of the discretized problem. To this end, consider the functions $\mathbf{F}_k : \mathbb{R}^n \rightarrow \mathbb{R}^n$ and $\mathbf{K}_k : \mathbb{R}^n \rightarrow \mathbb{R}^{n \times n}$ representing the vector of the internal forces and the consistent tangent stiffness matrix at the k -th step, respectively. Recall that $\mathbf{F}_k(\cdot)$ and $\mathbf{K}_k(\cdot)$ are assembled using values of the operators \mathbf{T} and \mathbb{T} at each integration point [2]. The algebraic representation of second and fourth order tensors is introduced in Appendix B.

Since we are interested in incremental limit analysis, we consider the external load vector $\mathbf{l} \in \mathbb{R}^n$ which is multiplied by a load factor $\zeta \in \mathbb{R}_+$. So the load vector in the k -th step reads as $\zeta_k \mathbf{l}$. It is convenient to distinguish two types of problems:

$$\begin{aligned} (\mathcal{P})_\zeta & \quad \text{given } \zeta_k \in \mathbb{R}_+, \text{ find } \mathbf{u}_k \in \mathbb{R}^n : \quad \mathbf{F}_k(\mathbf{u}_k) = \zeta_k \mathbf{l}, \\ (\mathcal{P})^\alpha & \quad \text{given } (\mathbf{b}, \alpha_k) \in \mathbb{R}^n \times \mathbb{R}_+, \text{ find } (\mathbf{u}_k, \zeta_k) \in \mathbb{R}^n \times \mathbb{R}_+ : \quad \begin{cases} \mathbf{F}_k(\mathbf{u}_k) = \zeta_k \mathbf{l}, \\ \mathbf{b}^T \mathbf{u}_k = \alpha_k. \end{cases} \end{aligned}$$

The former problem enables the direct control of the loading process through the load factor. This parameter is bounded from above by a limit value, ζ_{lim} , which is often finite (mainly in perfect plasticity). The limit value is an important safety parameter and beyond ζ_{lim} no solution exists. When the control through ζ is used the sequence

$$0 < \zeta_1 < \zeta_2 < \dots < \zeta_k < \zeta_{k+1} < \dots < \zeta_{lim}$$

is adaptively constructed to estimate ζ_{lim} . The adaptive strategy is usually based on convergence of a chosen numerical method to detect inadmissible load factors. Further, within the loading process, it is useful to investigate local and/or global material response such that the sequence $\{\alpha_k\}$, $\alpha_k = \mathbf{b}^T \mathbf{u}^k$, $k = 1, 2, \dots$, is computed using the solution \mathbf{u}^k to $(\mathcal{P})_\zeta$. There are many ways how to choose the vector \mathbf{b} to be the sequence $\{\alpha_k\}$ increasing. For example, one can detect a point on the investigated body where it is expected that the displacement is the most sensitive on the applied forces. In case of perfect plasticity, one can also set $\mathbf{b} = \mathbf{l}$. Such a choice represents the work of external forces, seems to be more universal and enables to analyze the convergence $h \rightarrow 0_+$ where h denotes the (space) discretization parameter [22, 23, 24, 25].

The problem $(\mathcal{P})^\alpha$ is inverse to $(\mathcal{P})_\zeta$ in sense that we prescribe $\{\alpha_k\}$ and compute the sequence $\{\zeta_k\}$. This leads to indirect control of the loading process. Here, we consider $(\mathcal{P})^\alpha$ mainly for the

nonassociative Mohr-Coulomb model where the sequence $\{\zeta_k\}$ need not be monotone. However, the indirect control has been successfully used also within associative perfect plasticity where $\zeta \rightarrow \zeta_{lim}$ as $\alpha \rightarrow +\infty$ [23, 24].

For solving $(\mathcal{P})_\zeta$ and $(\mathcal{P})^\alpha$ we introduce the semismooth Newton methods. For more details and convergence analysis, we refer, e.g., [23].

Algorithm 1 (ALG- ζ).

- 1: initialization: $\mathbf{u}_k^0 = \mathbf{u}_{k-1}$
- 2: **for** $i = 0, 1, 2, \dots$ **do**
- 3: find $\delta \mathbf{u}^i \in \mathbf{V}$: $\mathbf{K}_k(\mathbf{u}_k^i) \delta \mathbf{u}^i = \zeta_k \mathbf{l} - \mathbf{F}_k(\mathbf{u}_k^i)$
- 4: compute $\mathbf{u}_k^{i+1} = \mathbf{u}_k^i + \delta \mathbf{u}^i$
- 5: **if** $\|\delta \mathbf{u}^i\| / (\|\mathbf{u}_k^{i+1}\| + \|\mathbf{u}_k^i\|) \leq \epsilon_{Newton}$ **then stop**
- 6: **end for**
- 7: set $\mathbf{u}_k = \mathbf{u}_k^{i+1}$.

Algorithm 2 (ALG- α).

- 1: initialization: $\mathbf{u}_k^0 = \mathbf{u}_{k-1}$, $\zeta_k^0 = \zeta_{k-1}$
- 2: **for** $i = 0, 1, 2, \dots$ **do**
- 3: find $\mathbf{v}^i, \mathbf{w}^i \in \mathbf{V}$: $\tilde{\mathbf{K}}_k(\mathbf{u}_k^i) \mathbf{v}^i = \zeta_k^i \mathbf{l} - \mathbf{F}_k(\mathbf{u}_k^i)$, $\tilde{\mathbf{K}}_k(\mathbf{u}_k^i) \mathbf{w}^i = \mathbf{l}$
- 4: compute $\delta \zeta^i = [\alpha_k - \mathbf{b}^T(\mathbf{u}_k^i + \mathbf{v}^i)] / \mathbf{b}^T \mathbf{w}^i$
- 5: compute $\delta \mathbf{u}^i = \mathbf{v}^i + \delta \zeta^i \mathbf{w}^i$
- 6: set $\mathbf{u}_k^{i+1} = \mathbf{u}_k^i + \delta \mathbf{u}^i$, $\zeta_k^{i+1} = \zeta_k^i + \delta \zeta^i$
- 7: **if** $\|\delta \mathbf{u}^i\| / (\|\mathbf{u}_k^{i+1}\| + \|\mathbf{u}_k^i\|) \leq \epsilon_{Newton}$ **then stop**
- 8: **end for**
- 9: set $\mathbf{u}_k = \mathbf{u}_k^{i+1}$, $\zeta_k = \zeta_k^{i+1}$.

In ALG- α , the regularized stiffness matrix is used: $\tilde{\mathbf{K}}_k(\mathbf{u}_k^i) = (1 - r^i) \mathbf{K}_k(\mathbf{u}_k^i) + r^i \mathbf{K}_{el}$, where $r_i \rightarrow 0_+$ as $i \rightarrow +\infty$ and \mathbf{K}_{el} denotes the elastic stiffness matrix. It holds that $\mathbf{b}^T \mathbf{u}_k^{i+1} = \alpha_k$, $i = 0, 1, 2, \dots$. Notice that problem $(\mathcal{P})^\alpha$ and ALG- α is similar to arc-length methods introduced e.g. in [20, 1].

If \mathbf{T} is semismooth in $\mathbb{R}_{sym}^{3 \times 3}$ then \mathbf{F}_k is also semismooth in \mathbb{R}^n . The semismoothness is an essential assumption for local superlinear convergence of these algorithms. To observe such convergence, we set $\epsilon_{Newton} = 10^{-12}$ in all of the below introduced experiments.

7 Numerical experiments - slope stability

The improved return-mapping scheme for the Mohr-Coulomb model in combination with the semismooth Newton method have been implemented in MatLab for 3D slope stability problem and its plane strain reduction. These experimental codes denoted as SS-MC-NP-3D, SS-MC-NH and SS-MC-NP-Acontrol are vectorized and available in [26]. One can choose: a) several types of finite elements with appropriate numerical quadratures; b) locally refined meshes with various densities. Here, we confine mainly on results for the quadrilateral $Q2$ elements based on the expertise introduced in [2].

We consider the benchmark plane strain problem introduced in [1, Page 351] and its extension for 3D case. The 2D cross-section of the body with the coarsest mesh is depicted in Figure 1. The 3D geometry and the corresponding hexahedral mesh arise from 2D by extruding. The slope height is

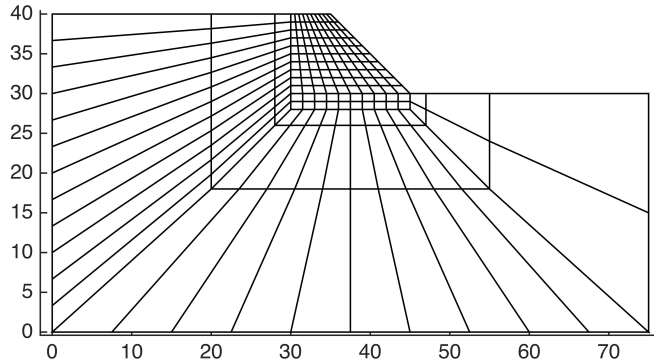


Figure 1: Cross section of the body with the coarsest mesh for $Q2$ elements.

10 m and its inclination is 45° . On the bottom, we assume that the body is fixed and, on the lateral sides, zero normal displacements are prescribed. The body is subjected to self-weight. We set the specific weight $\rho g = 20 \text{ kN/m}^3$ with ρ being the mass density and g the gravitational acceleration. Such a volume force is multiplied by the load factor, ζ . The parameter α is here the settlement at the corner point A on the top of the slope to be in accordance with [1]. Further, we set $E = 20\,000 \text{ kPa}$, $\nu = 0.49$, $\phi = 20^\circ$ and $c = 50 \text{ kPa}$, where c denotes the cohesion for the perfect plastic model. Hence, $G = 67\,114 \text{ kPa}$ and $K = 3\,333\,333 \text{ kPa}$. The remaining parameters for the Mohr-Coulomb model will be introduced below depending on a particular experiment.

We introduce three different experiments. The first and second experiments are related to the plane strain problem. The $Q2$ elements (i.e. eight-noded quadrilaterals) with 3×3 integration quadrature and hierarchy four levels of quadrilateral meshes with different densities are considered. The meshes have 627, 2405, 9417, and 37265 nodal points including the midpoints, see Figure 1, and 1728, 6912, 27648, and 110592 integration points, respectively. The third experiment is related to the 3D problem and the chosen elements and meshes are described below in Section 7.2.

7.1 Associative plane strain problem with nonlinear hardening

The aim of this experiment is to demonstrate efficiency of the code even if the constitutive solution cannot be found in closed form. Since the code contains a Matlab vectorization, we fix 10 inner Newton's iterations for finding the unknown plastic multipliers in each integration point. Algorithm ALG- ζ is used and the initial load increment $\delta\zeta = 0.1$ is considered. The loading process is stopped when the settlement is sufficiently large: $\alpha_k \geq 3 \text{ m}$. We set $\psi = \phi$ to have the associative model. The nonlinear hardening function is defined as it follows:

$$H(\bar{\varepsilon}^p) = \min \left\{ c - c_0, \tilde{H}\bar{\varepsilon}^p - \frac{\tilde{H}^2}{4(c - c_0)}(\bar{\varepsilon}^p)^2 \right\}, \quad c_0 = 40 \text{ kPa}, \quad \tilde{H} = 10000 \text{ kPa}.$$

Here, \tilde{H} represents the initial slope of the hardening function and the material response is perfect plastic for sufficiently large values of the hardening variable. One can easily check that the hardening function is smooth.

In Figure 2, dependence of the load paths on mesh density is introduced. We observe that the value ζ_{lim} decreases with increasing mesh density. For the finest mesh, ζ_{lim} seems to be very close to the theoretical bound 4.045 introduced in [27]. It is worth mentioning that we obtain practically the same curves for the related perfect plastic model with $c_0 = c = 50 \text{ kPa}$. The presented load curves are also comparable with the curve introduced in [1].

Figure 3 depicts numbers of Newton's iterations for each step k and the finest mesh. Up to Step 41 corresponding to $\zeta = 4$ and $\delta\zeta = 0.1$, the numbers of iterations are less than or equal to 15 which

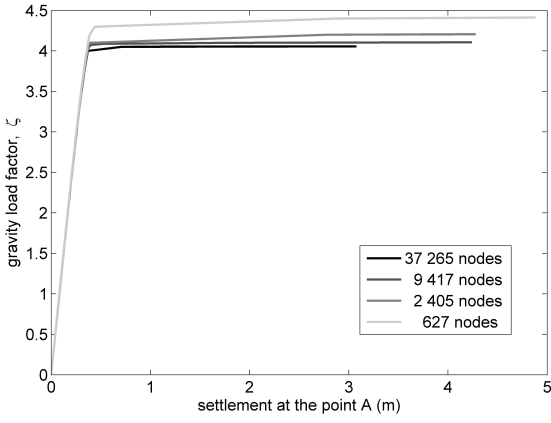


Figure 2: Load paths for different meshes.

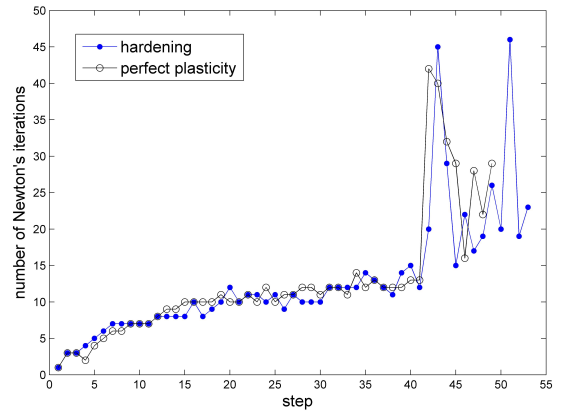


Figure 3: Numbers of iterations for each step k and the finest mesh.

is acceptable with respect to the mesh density. For Steps 42-53 with ζ close to ζ_{lim} and decreasing $\delta\zeta$, the numbers of iterations oscillate depending on the adaptive choice of ζ_k . This is caused by the fact that the small change of the load factor can cause large increment of the settlement. To exclude influence of the inexact constitutive solver on the numbers of iterations, we repeat this experiment for $c_0 = c = 50$ kPa, i.e., for the perfectly plastic model where one can find the constitutive solution in closed form. The comparison is also depicted in Figure 3. One can observe that the numbers of Newton's iteration are similar. We need only 48 steps to achieve the required settlement in case of perfect plasticity. Finally, notice that the superlinear convergence is observed in each step within a few last iterations.

7.2 Nonassociative perfect plastic plane strain problem

This experiment is performed to demonstrate that the load factor need not be increasing during the loading process controlled through α when $\psi < \phi$. In particular, we set $\psi = 5^\circ$ and $c_0 = c = 50$ kPa, i.e., $H = 0$. Further, it is considered ALG- α and the initial increment $\delta\alpha = 0.05$ m of the settlement.

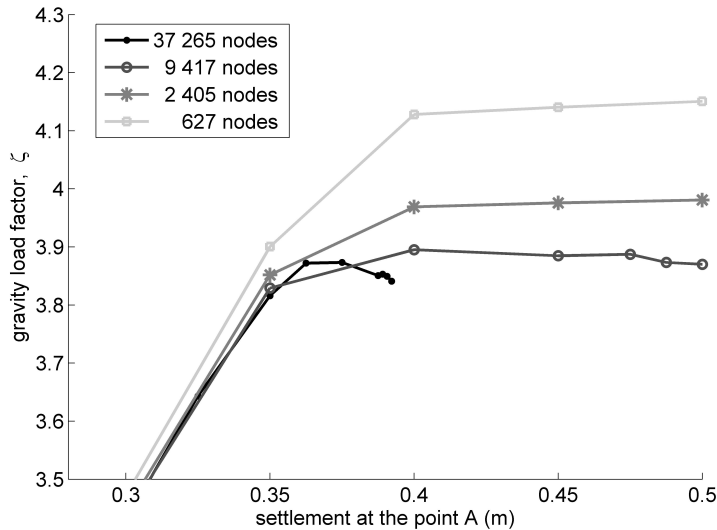


Figure 4: Comparison of the loading paths for $\psi = 5^\circ$. Zoom of the curves in vicinity of the limit load.

In Figure 4, the load curves for the investigated meshes are depicted. We see only their details in vicinity of the limit load. For two coarsest meshes, one can let $\delta\alpha = 0.05$ m up to $\alpha_{max} = 3$ m

and the computed sequences $\{\zeta_k\}$ remain monotone. However, for two finest meshes, $\{\zeta_k\}$ are not monotone. Moreover, to find iterative solutions for α larger, it was necessary to decrease $\delta\alpha$ and the value α_{max} was not achieved. We observe that the slope of the “post-peak” branch strongly depends on the mesh density. As in the previous experiment, ζ_{lim} decreases with increasing mesh density.

7.3 Associative perfect plastic 3D problem

In [2], strong dependence of the mesh density on incremental limit analysis for the $P1$ elements (linear tetrahedrons) and the plane strain problem was emphasized. For the 3D problem, this dependence seems to be more dramatic. For example, we observe that for the $P1$ elements the loading curves are not bounded from above. Therefore, we focus on comparison of the loading paths for the $Q1$ and $Q2$ elements (i.e. 8-noded and 20-noded hexahedrons). We consider $2 \times 2 \times 2$ and $3 \times 3 \times 3$ noded integration quadratures for these element types, respectively. Two hexahedral meshes are prepared for this experiment. For the $Q1$ elements, the meshes contain 5103 and 37597 nodal points, 34560 and 276480 integration points, respectively. For the $Q2$ elements, the meshes contain 19581 and 147257 nodal points, 116640 and 933120 integration points, respectively. The loading process is stopped when the settlement is sufficiently large: $\alpha_k \geq 5$ m.

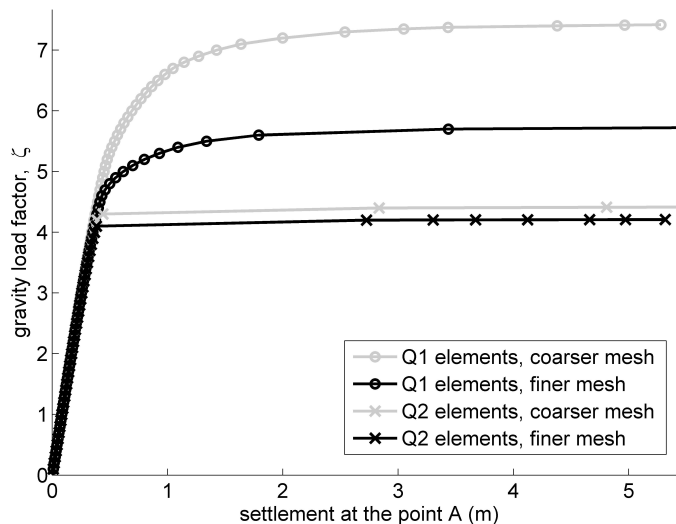


Figure 5: Comparison of the loading paths for $Q1$ and $Q2$ elements.

The corresponding loading paths obtained by ALG- ζ are depicted in Figure 5. We observe that the estimated limit values of ζ are close to the expected value of 4.045 for the $Q2$ elements but not for the $Q1$ elements. To estimate ζ_{lim} using the $Q1$ elements, it would be necessary to use much finer meshes. Figures 6 and 7 illustrate failure at the end of the loading process for the $Q2$ elements and the finer mesh.

8 Conclusion

The main idea of this paper is based on the subdifferential formulation of the plastic flow rule and its using for computational purposes and numerical analysis. This was illustrated on the model containing the Mohr-Coulomb yield criterion, a nonassociative plastic flow rule and a nonlinear isotropic hardening. Closed form to the subdifferential of the plastic potential was derived at first. This auxiliary result leads to simpler construction of the constitutive solution and the consistent tangent operator. In comparison to the conventional Koiter formulations, the new technique enables to

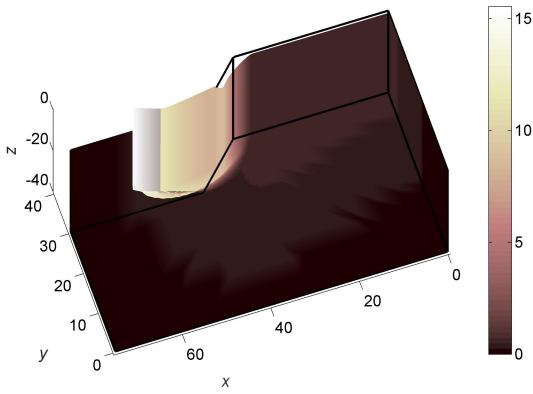


Figure 6: Total displacement and deformed shape at the end of the loading process.

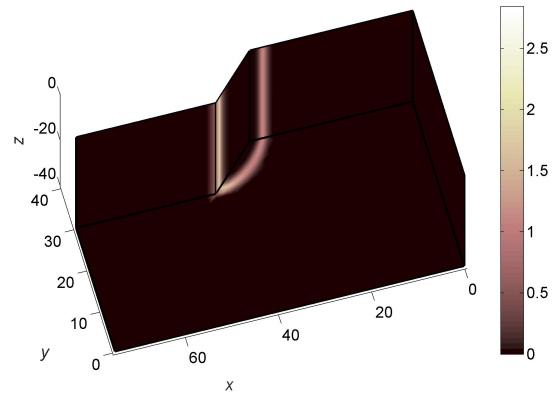


Figure 7: Plastic multipliers at the end of the loading process.

a priori decide which type of the return on the yield surface happens even if the constitutive solution cannot be found in closed form. Further, the dependence of the unknown principal stresses on the trial principal stresses was described in detail. This leads to the reduction of “branching” within the construction of the consistent tangent operator in comparison to [1]. The derived constitutive formulas could be also used to show that the stress-strain operator is semismooth.

The improved constitutive solution was tested within incremental limit analysis related to the slope stability problem in 2D and 3D. Beside the conventional incremental boundary value elastoplastic problem, an auxiliary problem enabling indirect control of the loading process was also considered. For both the problems, the semismooth Newton method was introduced. We focused on the efficiency of the presented numerical solution, the dependence of the loading curves on mesh density and type of finite elements within numerical experiments.

The main idea seems to be more universal. In [2], it was successfully used to simplify constitutive solution schemes for potentials that are isotropic and independent of the Lode angle. The extension of the results seems to be straightforward for a similar model with the Tresca yield criterion.

Acknowledgements

The authors would like to thank to Pavel Maršálek for generating the quadrilateral meshes with and without midpoints in 2D and 3D. This work was supported by The Ministry of Education, Youth and Sports from the National Programme of Sustainability (NPU II), project “IT4Innovations excellence in science - LQ1602”.

Appendix

A. Simplified constitutive handling for the plane strain problem

The results of Section 4 and 5 are, of course, valid also for the plane strain problem. Nevertheless, in this case, one can simplify the forms of eigenprojections and their derivatives since we work only on the subspace \mathbb{R}_{PS} of $\mathbb{R}_{sym}^{3 \times 3}$ containing trial tensors in the form

$$\boldsymbol{\varepsilon} = \begin{pmatrix} \varepsilon_{11} & \varepsilon_{12} & 0 \\ \varepsilon_{12} & \varepsilon_{22} & 0 \\ 0 & 0 & \varepsilon_{33} \end{pmatrix}.$$

To distinguish the derivatives of functions defined in \mathbb{R}_{PS} , we use the symbol $\tilde{\mathcal{D}}$ instead of \mathcal{D} . Define the functions

$$\begin{aligned}\tilde{\omega}_1(\boldsymbol{\varepsilon}) &:= \frac{1}{2} \left[\varepsilon_{11} + \varepsilon_{22} + \sqrt{(\varepsilon_{11} - \varepsilon_{22})^2 + 4\varepsilon_{12}^2} \right], \\ \tilde{\omega}_2(\boldsymbol{\varepsilon}) &:= \frac{1}{2} \left[\varepsilon_{11} + \varepsilon_{22} - \sqrt{(\varepsilon_{11} - \varepsilon_{22})^2 + 4\varepsilon_{12}^2} \right], \\ \tilde{\omega}_3(\boldsymbol{\varepsilon}) &:= \varepsilon_{33}\end{aligned}$$

in \mathbb{R}_{PS} . Then $\tilde{\varepsilon}_i = \tilde{\omega}_i(\boldsymbol{\varepsilon})$, $i = 1, 2, 3$, are the eigenvalues of $\boldsymbol{\varepsilon}$. These values are not ordered in general. We only know that $\tilde{\varepsilon}_1 \geq \tilde{\varepsilon}_2$. Further, define

$$\begin{aligned}\tilde{\boldsymbol{\varepsilon}}(\boldsymbol{\varepsilon}) &:= \begin{pmatrix} \varepsilon_{11} & \varepsilon_{12} & 0 \\ \varepsilon_{12} & \varepsilon_{22} & 0 \\ 0 & 0 & 0 \end{pmatrix}, \quad \tilde{\mathbf{I}} := \begin{pmatrix} 1 & 0 & 0 \\ 0 & 1 & 0 \\ 0 & 0 & 0 \end{pmatrix}, \quad \tilde{\mathbf{E}}_3(\boldsymbol{\varepsilon}) := \begin{pmatrix} 0 & 0 & 0 \\ 0 & 0 & 0 \\ 0 & 0 & 1 \end{pmatrix}, \\ \tilde{\mathbf{E}}_1(\boldsymbol{\varepsilon}) &:= \begin{cases} \frac{\tilde{\varepsilon}_1 - \tilde{\varepsilon}_2 \tilde{\mathbf{I}}}{\tilde{\varepsilon}_1 - \tilde{\varepsilon}_2}, & \tilde{\varepsilon}_1 > \tilde{\varepsilon}_2 \\ \tilde{\mathbf{I}}, & \tilde{\varepsilon}_1 = \tilde{\varepsilon}_2 \end{cases}, \quad \tilde{\mathbf{E}}_2(\boldsymbol{\varepsilon}) := \tilde{\mathbf{I}} - \tilde{\mathbf{E}}_1(\boldsymbol{\varepsilon})\end{aligned}$$

and

$$\tilde{\mathbb{E}}_1(\boldsymbol{\varepsilon}) := \begin{cases} \frac{1}{\tilde{\varepsilon}_1 - \tilde{\varepsilon}_2} [\tilde{\mathbb{I}} - \tilde{\mathbf{E}}_1 \otimes \tilde{\mathbf{E}}_1 - \tilde{\mathbf{E}}_2 \otimes \tilde{\mathbf{E}}_2], & \tilde{\varepsilon}_1 > \tilde{\varepsilon}_2 \\ \mathbb{O}, & \tilde{\varepsilon}_1 = \tilde{\varepsilon}_2 \end{cases}, \quad \tilde{\mathbb{E}}_2(\boldsymbol{\varepsilon}) := -\tilde{\mathbb{E}}_1(\boldsymbol{\varepsilon}), \quad \tilde{\mathbb{E}}_3(\boldsymbol{\varepsilon}) := \mathbb{O},$$

where \mathbb{O} denotes the zeroth fourth order tensor and $[\tilde{\mathbb{I}}]_{ijkl} = \delta_{ik}\delta_{jl}$, $i, j, k, l = 1, 2$, otherwise $[\tilde{\mathbb{I}}]_{ijkl} = 0$. Clearly, $\mathcal{D}\tilde{\omega}_3(\boldsymbol{\varepsilon}) = \tilde{\mathcal{D}}\tilde{\omega}_3(\boldsymbol{\varepsilon}) = \tilde{\mathbf{E}}_3(\boldsymbol{\varepsilon})$. If $\tilde{\varepsilon}_1 > \tilde{\varepsilon}_2$ then

$$\tilde{\mathbf{E}}_i(\boldsymbol{\varepsilon}) = \tilde{\mathcal{D}}\tilde{\omega}_i(\boldsymbol{\varepsilon}), \quad \tilde{\mathbb{E}}_i(\boldsymbol{\varepsilon}) = \tilde{\mathcal{D}}\tilde{\mathbf{E}}_i(\boldsymbol{\varepsilon}) \quad \text{in } \mathbb{R}_{PS}, \quad i = 1, 2.$$

It is worth mentioning that these formulas need not hold in $\mathbb{R}_{sym}^{3 \times 3}$ in general. Similar formulas are also introduced in [1, Appendix A].

Now, it is necessary to reorder the eigenvalues of $\boldsymbol{\varepsilon} \in \mathbb{R}_{PS}$. Denote the ordered eigenvalues as $\varepsilon_1, \varepsilon_2, \varepsilon_3$, i.e., $\varepsilon_1 := \max\{\tilde{\varepsilon}_1, \tilde{\varepsilon}_3\}$ and $\varepsilon_3 := \min\{\tilde{\varepsilon}_2, \tilde{\varepsilon}_3\}$. Consequently, we reorder the functions $\tilde{\omega}_i$, $\tilde{\mathbf{E}}_i$, $\tilde{\mathbb{E}}_i$, $i = 1, 2, 3$, leading to the functions ω_i , \mathbf{E}_i , \mathbb{E}_i , $i = 1, 2, 3$. To complete the notation, one can easily set

$$\mathbf{E}_{12}(\boldsymbol{\varepsilon}) := \mathbf{E}_1(\boldsymbol{\varepsilon}) + \mathbf{E}_2(\boldsymbol{\varepsilon}), \quad \mathbf{E}_{23}(\boldsymbol{\varepsilon}) := \mathbf{E}_2(\boldsymbol{\varepsilon}) + \mathbf{E}_3(\boldsymbol{\varepsilon}) \quad \forall \boldsymbol{\varepsilon} \in \mathbb{R}_{PS}.$$

Finally, one can straightforwardly use the functions ω_i , \mathbf{E}_i , \mathbb{E}_i , $i = 1, 2, 3$, \mathbf{E}_{12} and \mathbf{E}_{23} within Section 5 when the plane strain assumptions are considered.

B. Algebraic representation of second and fourth order tensors

Within our implementation, we use the standard algebraic representation of stress and strain second order tensors specified below but a little bit different representation of fourth order tensors in comparison to [1, Appendix D]. We assume that a fourth order tensor \mathbb{C} represents a linear mapping from $\mathbb{R}_{sym}^{3 \times 3}$ into $\mathbb{R}_{sym}^{3 \times 3}$. Therefore, the components $[\mathbb{C}]_{ijkl} \equiv C_{ijkl}$ of \mathbb{C} satisfy

$$\sum_{k,l} C_{ijkl} \eta_{kl} = \sum_{k,l} C_{jikl} \eta_{kl} \quad \forall \boldsymbol{\eta} \in \mathbb{R}_{sym}^{3 \times 3}, \quad \eta_{kl} = [\boldsymbol{\eta}]_{kl}.$$

The choice $\eta_{kl} = \delta_{mk}\delta_{nl} + \delta_{nk}\delta_{ml}$ implies that $\boldsymbol{\eta} \in \mathbb{R}_{sym}^{3 \times 3}$ for any $m, n = 1, 2, 3$ and

$$C_{ijmn} + C_{ijnm} = C_{jimn} + C_{jinm} \quad \forall i, j, m, n = 1, 2, 3. \quad (\text{B.1})$$

Notice that in [1, Appendix D], the stronger assumptions on the components are required: $C_{ijmn} = C_{ijnm} = C_{jimn} = C_{jinm}$.

We distinguish two cases: the 3D problem and its plane strain reduction.

The 3D problem

Let $\boldsymbol{\tau}, \boldsymbol{\eta} \in \mathbb{R}_{sym}^{3 \times 3}$ denote stress and strain tensors, respectively. Then they are represented by vectors $\mathbf{t} = (\tau_{11}, \tau_{22}, \tau_{33}, \tau_{12}, \tau_{23}, \tau_{13})^T$ and $\mathbf{n} = (\eta_{11}, \eta_{22}, \eta_{33}, 2\eta_{12}, 2\eta_{23}, 2\eta_{13})^T$ where τ_{ij} and η_{ij} are the components of $\boldsymbol{\tau}$, and $\boldsymbol{\eta}$, respectively. Clearly, $\boldsymbol{\tau} : \boldsymbol{\eta} = \mathbf{t} \cdot \mathbf{n}$. A fourth order tensor \mathbb{C} is represented by matrix $\mathbf{C} \in \mathbb{R}^{6 \times 6}$. Since fourth order tensors are applied on strain tensors within the implementation, we require that

$$\boldsymbol{\eta} : \mathbb{C} : \boldsymbol{\varepsilon} = \mathbf{n} \cdot \mathbf{C} \mathbf{e} \quad (\text{B.2})$$

holds for any strain tensors $\boldsymbol{\eta}$ and $\boldsymbol{\varepsilon}$. Here, \mathbf{n} and \mathbf{e} denote the algebraic counterparts of $\boldsymbol{\eta}$ and $\boldsymbol{\varepsilon}$, respectively. From (B.1) and (B.2), one can derive that

$$\mathbf{C} = \begin{pmatrix} C_{1111} & C_{1122} & C_{1133} & \frac{1}{2}[C_{1112} + C_{1121}] & \frac{1}{2}[C_{1123} + C_{1132}] & \frac{1}{2}[C_{1113} + C_{1131}] \\ C_{2211} & C_{2222} & C_{2233} & \frac{1}{2}[C_{2212} + C_{2221}] & \frac{1}{2}[C_{2223} + C_{2232}] & \frac{1}{2}[C_{2213} + C_{2231}] \\ C_{3311} & C_{3322} & C_{3333} & \frac{1}{2}[C_{3312} + C_{3321}] & \frac{1}{2}[C_{3323} + C_{3332}] & \frac{1}{2}[C_{3313} + C_{3331}] \\ C_{1211} & C_{1222} & C_{1233} & \frac{1}{2}[C_{1212} + C_{1221}] & \frac{1}{2}[C_{1223} + C_{1232}] & \frac{1}{2}[C_{1213} + C_{1231}] \\ C_{2311} & C_{2322} & C_{2333} & \frac{1}{2}[C_{2312} + C_{2321}] & \frac{1}{2}[C_{2323} + C_{2332}] & \frac{1}{2}[C_{2313} + C_{2331}] \\ C_{1311} & C_{1322} & C_{1333} & \frac{1}{2}[C_{1312} + C_{1321}] & \frac{1}{2}[C_{1323} + C_{1332}] & \frac{1}{2}[C_{1313} + C_{1331}] \end{pmatrix}.$$

Indeed, the choices $\varepsilon_{kl} = \frac{1}{2}(\delta_{2k}\delta_{3l} + \delta_{2l}\delta_{3k})$, $\eta_{ij} = \frac{1}{2}(\delta_{1i}\delta_{2j} + \delta_{2i}\delta_{1j})$ imply $\mathbf{e} = (0, 0, 0, 0, 1, 0)^T$ and $\mathbf{n} = (0, 0, 0, 1, 0, 0)^T$. Hence,

$$[\mathbf{C}]_{45} = \mathbf{n} \cdot \mathbf{C} \mathbf{e} \stackrel{(B.2)}{=} \boldsymbol{\eta} : \mathbb{C} : \boldsymbol{\varepsilon} = \frac{1}{4}[C_{1223} + C_{1232} + C_{2123} + C_{2132}] \stackrel{(B.1)}{=} \frac{1}{2}[C_{1223} + C_{1232}].$$

Similarly, one can derive the forms of other components of \mathbf{C} . Notice that the algebraic representation of \mathbb{C} is more general than in [1, Appendix D].

We introduce three examples useful for the Mohr-Coulomb model:

1. Let $\mathbb{C} = \mathbb{I}$. Then $C_{ijkl} = \delta_{ik}\delta_{jl}$ and $\mathbf{C} = \text{diag}(1, 1, 1, 1/2, 1/2, 1/2)$. Notice that the same matrix is derived in [1, Appendix D] although the tensor \mathbb{I}_S , $[\mathbb{I}_S]_{ijkl} = \frac{1}{2}(\delta_{ik}\delta_{jl} + \delta_{il}\delta_{jk})$, is used there instead of \mathbb{I} .
2. Let $\mathbb{C} = \boldsymbol{\tau} \otimes \boldsymbol{\sigma}$ where $\boldsymbol{\sigma}, \boldsymbol{\tau}$ are arbitrary chosen stress tensors. Denote \mathbf{s} and \mathbf{t} as the algebraic counterparts to $\boldsymbol{\sigma}, \boldsymbol{\tau}$, respectively. Then $\mathbf{C} = \mathbf{s} \mathbf{t}^T$.
3. Let $\mathbb{C} = \mathcal{D}(\boldsymbol{\eta}^2)$. Then $C_{ijkl} = \delta_{ik}\eta_{lj} + \delta_{jl}\eta_{ik}$ and

$$\mathbf{C} = \begin{pmatrix} 2\eta_{11} & 0 & 0 & \eta_{12} & 0 & \eta_{13} \\ 0 & 2\eta_{22} & 0 & \eta_{12} & \eta_{23} & 0 \\ 0 & 0 & 2\eta_{33} & 0 & \eta_{23} & \eta_{13} \\ \eta_{12} & \eta_{12} & 0 & \frac{1}{2}[\eta_{11} + \eta_{22}] & \frac{1}{2}\eta_{13} & \frac{1}{2}\eta_{23} \\ 0 & \eta_{23} & \eta_{23} & \frac{1}{2}\eta_{13} & \frac{1}{2}[\eta_{22} + \eta_{33}] & \frac{1}{2}\eta_{12} \\ \eta_{13} & 0 & \eta_{13} & \frac{1}{2}\eta_{23} & \frac{1}{2}\eta_{12} & \frac{1}{2}[\eta_{11} + \eta_{33}] \end{pmatrix}.$$

The plane strain problem

Let $\boldsymbol{\tau}$ and $\boldsymbol{\eta}$ denote stress and strain second order tensors, respectively. Then they are represented by the vectors $\mathbf{t} = (\tau_{11}, \tau_{22}, \tau_{12}, \tau_{33})^T$ and $\mathbf{n} = (\eta_{11}, \eta_{22}, 2\eta_{12}, \eta_{33})^T$ where τ_{ij} and η_{ij} are components of $\boldsymbol{\tau}$, and $\boldsymbol{\eta}$, respectively. Clearly, $\boldsymbol{\tau} : \boldsymbol{\eta} = \mathbf{t} \cdot \mathbf{n}$. Notice that the component η_{33} vanishes for the strain tensor but not for the plastic strain tensor.

The fourth order tensor \mathbb{C} can be represented by matrix $\mathbf{C} \in \mathbb{R}^{4 \times 4}$. Similarly as for the 3D problem, one can derive that

$$\mathbf{C} = \begin{pmatrix} C_{1111} & C_{1122} & \frac{1}{2}[C_{1112} + C_{1121}] & C_{1133} \\ C_{2211} & C_{2222} & \frac{1}{2}[C_{2212} + C_{2221}] & C_{2233} \\ C_{1211} & C_{1222} & \frac{1}{2}[C_{1212} + C_{1221}] & C_{1233} \\ C_{3311} & C_{3322} & \frac{1}{2}[C_{3312} + C_{3321}] & C_{3333} \end{pmatrix}.$$

Finally, it is worth mentioning that for assembling the tangent stiffness matrix, it is sufficient to save only the components $(\mathbf{C})_{ij}$ where $i, j = 1, 2, 3$.

References

- [1] de Souza Neto EA, Peri D, Owen DRJ. *Computational Methods for Plasticity*. Wiley-Blackwell, 2008, doi:10.1002/9780470694626. URL <http://dx.doi.org/10.1002/9780470694626>.
- [2] Sysala S, Cermak M, Koudelka T, Kruis J, Zeman J, Blaheta R. An improved return-mapping scheme for nonsmooth yield surfaces: PART I - the Haigh-Westergaard coordinates. Submitted, 2015, <http://arxiv.org/abs/1503.03605>.
- [3] Gruber PG, Valdman J. Solution of one-time-step problems in elastoplasticity by a slant Newton method. *SIAM J. Sci. Comput.* jan 2009; **31**(2):1558–1580, doi:10.1137/070690079. URL <http://dx.doi.org/10.1137/070690079>.
- [4] Sauter M, Wieners C. On the superlinear convergence in computational elasto-plasticity. *Computer Methods in Applied Mechanics and Engineering* dec 2011; **200**(49-52):3646–3658, doi:10.1016/j.cma.2011.08.011. URL <http://dx.doi.org/10.1016/j.cma.2011.08.011>.
- [5] Sysala S. Application of a modified semismooth Newton method to some elasto-plastic problems. *Mathematics and Computers in Simulation* jun 2012; **82**(10):2004–2021, doi:10.1016/j.matcom.2012.03.012. URL <http://dx.doi.org/10.1016/j.matcom.2012.03.012>.
- [6] Sysala S. Properties and simplifications of constitutive time-discretized elastoplastic operators. *ZAMM - Journal of Applied Mathematics and Mechanics / Zeitschrift für Angewandte Mathematik und Mechanik* feb 2014; **94**(3):233–255, doi:10.1002/zamm.201200056. URL <http://dx.doi.org/10.1002/zamm.201200056>.
- [7] Clausen J, Damkilde L, Andersen LV. Robust and efficient handling of yield surface discontinuities in elasto-plastic finite element calculations. *Engineering Computations* aug 2015; **32**(6):1722–1752, doi:10.1108/ec-01-2014-0008. URL <http://dx.doi.org/10.1108/EC-01-2014-0008>.
- [8] Lin C, Li YM. A return mapping algorithm for unified strength theory model. *International Journal for Numerical Methods in Engineering* jun 2015; **104**(8):749–766, doi:10.1002/nme.4937. URL <http://dx.doi.org/10.1002/nme.4937>.
- [9] Borja RI, Sama KM, Sanz PF. On the numerical integration of three-invariant elastoplastic constitutive models. *Computer Methods in Applied Mechanics and Engineering* feb 2003; **192**(9-10):1227–1258, doi:10.1016/s0045-7825(02)00620-5. URL [http://dx.doi.org/10.1016/S0045-7825\(02\)00620-5](http://dx.doi.org/10.1016/S0045-7825(02)00620-5).

- [10] Karaoulanis FE. Implicit numerical integration of nonsmooth multisurface yield criteria in the principal stress space. *Arch Computat Methods Eng* jul 2013; **20**(3):263–308, doi:10.1007/s11831-013-9087-3. URL <http://dx.doi.org/10.1007/s11831-013-9087-3>.
- [11] Koiter WT. Stress-strain relations, uniqueness and variational theorems for elastic-plastic materials with a singular yield surface. *Quarterly of Applied Mathematics* 1953; **11**(3):350–354. URL <http://www.jstor.org/stable/43634060>.
- [12] de Borst R. Integration of plasticity equations for singular yield functions. *Computers & Structures* jan 1987; **26**(5):823–829, doi:10.1016/0045-7949(87)90032-0. URL [http://dx.doi.org/10.1016/0045-7949\(87\)90032-0](http://dx.doi.org/10.1016/0045-7949(87)90032-0).
- [13] Han W, Reddy BD. *Plasticity: mathematical theory and numerical analysis*. Springer-Verlag, 1999, doi:10.1007/b97851. URL <http://dx.doi.org/10.1007/b97851>.
- [14] Berga A. Mathematical and numerical modeling of the non-associated plasticity of soils—part 1: The boundary value problem. *International Journal of Non-Linear Mechanics* jan 2012; **47**(1):26–35, doi:10.1016/j.ijnonlinmec.2011.08.008. URL <http://dx.doi.org/10.1016/j.ijnonlinmec.2011.08.008>.
- [15] Simo JC, Hughes TJ. *Computational inelasticity*, vol. 7. Springer Science & Business Media, 2006.
- [16] Starman B, Halilović M, Vrh M, Štok B. Consistent tangent operator for cutting-plane algorithm of elasto-plasticity. *Computer Methods in Applied Mechanics and Engineering* apr 2014; **272**:214–232, doi:10.1016/j.cma.2013.12.012. URL <http://dx.doi.org/10.1016/j.cma.2013.12.012>.
- [17] Clausen J, Damkilde L, Andersen L. Efficient return algorithms for associated plasticity with multiple yield planes. *International Journal for Numerical Methods in Engineering* 2006; **66**(6):1036–1059, doi:10.1002/nme.1595. URL <http://dx.doi.org/10.1002/nme.1595>.
- [18] Čermák M, Kozubek T, Sysala S, Valdman J. A TFETI domain decomposition solver for elastoplastic problems. *Applied Mathematics and Computation* mar 2014; **231**:634–653, doi:10.1016/j.amc.2013.12.186. URL <http://dx.doi.org/10.1016/j.amc.2013.12.186>.
- [19] Carlson DE, Hoger A. The derivative of a tensor-valued function of a tensor. *The Quarterly of Applied Mathematics* 1986; **44**:409–423.
- [20] de Borst R, Crisfield MA, Remmers JJC, Verhoosel CV. *Non-Linear Finite Element Analysis of Solids and Structures*. Wiley-Blackwell, 2012, doi:10.1002/9781118375938. URL <http://dx.doi.org/10.1002/9781118375938>.
- [21] Abbo A, Lyamin A, Sloan S, Hambleton J. A C2 continuous approximation to the Mohr–Coulomb yield surface. *International Journal of Solids and Structures* oct 2011; **48**(21):3001–3010, doi:10.1016/j.ijsolstr.2011.06.021. URL <http://dx.doi.org/10.1016/j.ijsolstr.2011.06.021>.
- [22] Sysala S, Haslinger J, Hlaváček I, Cermak M. Discretization and numerical realization of contact problems for elastic-perfectly plastic bodies. PART I - discretization, limit analysis. *ZAMM - Journal of Applied Mathematics and Mechanics / Zeitschrift für Angewandte Mathematik und Mechanik* nov 2013; **95**(4):333–353, doi:10.1002/zamm.201300112. URL <http://dx.doi.org/10.1002/zamm.201300112>.

- [23] Cermak M, Haslinger J, Kozubek T, Sysala S. Discretization and numerical realization of contact problems for elastic-perfectly plastic bodies. PART II - numerical realization, limit analysis. *ZAMM - Journal of Applied Mathematics and Mechanics / Zeitschrift für Angewandte Mathematik und Mechanik* jan 2015; **95**(12):1348–1371, doi:10.1002/zamm.201400069. URL <http://dx.doi.org/10.1002/zamm.201400069>.
- [24] Haslinger J, Repin S, Sysala S. A reliable incremental method of computing the limit load in deformation plasticity based on compliance: Continuous and discrete setting. *Journal of Computational and Applied Mathematics* sep 2016; **303**:156–170, doi:10.1016/j.cam.2016.02.035. URL <http://dx.doi.org/10.1016/j.cam.2016.02.035>.
- [25] Haslinger J, Repin S, Sysala S. Guaranteed and computable bounds of the limit load for variational problems with linear growth energy functionals. Submitted, 2016.
- [26] Sysala S, Cermak M. Experimental matlab code for the slope stability benchmark – SS-MC-NP-3D, SS-MC-NH, SS-MC-NP-Acontrol 2016. URL www.ugn.cas.cz/?p=publish/output.php, (or www.ugn.cas.cz - Publications - Other outputs - SS-MC-NP-3D, SS-MC-NH, SS-MC-NP-Acontrol).
- [27] Chen WF, Liu XL. Limit analysis in soil mechanics. *Limit analysis in soil mechanics* 1990; URL www.scopus.com.